Feedback Inhibition of Starch Degradation in Arabidopsis Leaves Mediated by Trehalose 6-Phosphate[1][W][OPEN]

Marina Camara Mattos Martins[2], Mahdi Hejazi, Joerg Fettke, Martin Steup, Regina Feil, Ursula Krause, Stéphanie Arrivault, Daniel Vosloh[3], Carlos María Figueroa, Alexander Ivakov, Umesh Prasad Yadav[4], Maria Piques, Daniela Metzner, Mark Stitt, and John Edward Lunn*

Max Planck Institute of Molecular Plant Physiology, Wissenschaftspark Golm, 14476 Potsdam-Golm, Germany (M.C.M.M., R.F., U.K., S.A., D.V., C.M.F., A.I., U.P.Y., M.P., D.M., M.Sti., J.E.L.); and Institute of Biochemistry and Biology, Department of Plant Physiology, University of Potsdam, 14476 Potsdam-Golm, Germany (M.H., J.F., M.Ste.)

Many plants accumulate substantial starch reserves in their leaves during the day and remobilize them at night to provide carbon and energy for maintenance and growth. In this paper, we explore the role of a sugar-signaling metabolite, trehalose-6-phosphate (Tre6P), in regulating the accumulation and turnover of transitory starch in Arabidopsis (*Arabidopsis thaliana*) leaves. Ethanol-induced overexpression of trehalose-phosphate synthase during the day increased Tre6P levels up to 11-fold. There was a transient increase in the rate of starch accumulation in the middle of the day, but this was not linked to reductive activation of ADP-glucose pyrophosphorylase. A 2- to 3-fold increase in Tre6P during the night led to significant inhibition of starch degradation. Maltose and maltotriose did not accumulate, suggesting that Tre6P affects an early step in the pathway of starch degradation in the chloroplasts. Starch granules isolated from induced plants had a higher orthophosphate content than granules from noninduced control plants, consistent either with disruption of the phosphorylation-dephosphorylation cycle that is essential for efficient starch breakdown or with inhibition of starch hydrolysis by β-amylase. Nonaqueous fractionation of leaves showed that Tre6P is predominantly located in the cytosol, with estimated in vivo Tre6P concentrations of 4 to 7 μM in the cytosol, 0.2 to 0.5 μM in the chloroplasts, and 0.05 μM in the vacuole. It is proposed that Tre6P is a component in a signaling pathway that mediates the feedback regulation of starch breakdown by sucrose, potentially linking starch turnover to demand for sucrose by growing sink organs at night.

Starch and Suc are the main products of photosynthesis in higher plants (Stitt et al., 2010). Much of the Suc synthesized during the day is exported from the leaves to support the growth of heterotrophic sink organs, whereas starch accumulates in the leaves during the day. This starch is then broken down at night to provide substrates for leaf respiration and Suc synthesis, allowing Suc export to continue in the dark. In this way, the transitory starch reserves in the leaf enable the plant to meet the daily challenge of surviving and growing through the night when photosynthesis is no longer possible. The efficient management of these reserves is essential if the plant is to optimize its growth rates and achieve reproductive success (Smith and Stitt, 2007; Andriotis et al., 2012; Stitt and Zeeman, 2012). In this paper, we explore the role of a sugar signaling metabolite, trehalose-6-phosphate (Tre6P), in regulating the accumulation and/or turnover of transitory starch in Arabidopsis (*Arabidopsis thaliana*) leaves, potentially linking the management of these reserves to the availability and demand for Suc.

In leaves, starch and Suc are ultimately synthesized from intermediates of the Calvin-Benson cycle, and the total flux into these end products is closely coordinated with the net rate of CO_2 assimilation (Stitt et al., 2010). From the fluctuations in metabolite levels observed in leaves during the diurnal cycle and in vitro studies of enzyme properties, a model was developed to explain how various regulatory mechanisms are integrated to bring about feed-forward or feedback regulation of Suc synthesis and photoassimilate partitioning (for review, see MacRae and Lunn, 2006). This model considers starch to be an "overflow" product

[1] This work was supported by a Ph.D. fellowship (to M.C.M.M.) from the Coordenação de Aperfeiçoamento de Pessoal de Nível Superior Brazil (grant no. BEX2762/07–2) and the Deutscher Akademischer Austauschdienst (grant no. A/07/70615), the Deutsche Forschungsgemeinschaft (grant no. SFB 429 to M.H, J.F., M.Ste., A.I., M.Sti., and J.E.L.), the European Commission FP7 collaborative project TiMet (contract no. 245142 to M.Sti.), and the Max Planck Society.

[2] Present address: Brazilian Bioethanol Science and Technology Laboratory, Rua Giuseppe Máximo Scolfaro, 10.000-Bairro Guará, Barão Geraldo, Campinas, CP 6192, 13083–970, Brazil.

[3] Present address: Institute for Plant Biotechnology, Stellenbosch University, Private Bag X1, Matieland 7602, South Africa.

[4] Present address: University of North Texas, Department of Biological Sciences, 1155 Union Circle #305220, Denton, TX 76203–5017.

* Address correspondence to lunn@mpimp-golm.mpg.de.

The author responsible for distribution of materials integral to the findings presented in this article in accordance with the policy described in the Instructions for Authors (www.plantphysiol.org) is: John E. Lunn (lunn@mpimp-golm.mpg.de).

[W] The online version of this article contains Web-only data.

[OPEN] Articles can be viewed online without a subscription.

www.plantphysiol.org/cgi/doi/10.1104/pp.113.226787

that is synthesized from surplus photoassimilate when photosynthesis exceeds the capacity of the leaves to export or store Suc (Cseke et al., 1994). According to the model, rising levels of Suc result in progressive inactivation of sucrose-phosphate synthase (SPS; Stitt et al., 1988). This triggers a cascade of events, including inhibition of the cytosolic Fru-1,6-bisphosphatase by rising levels of Fru-2,6-bisP, that coordinately decrease flux through the whole pathway of Suc synthesis and, therefore, the release of orthophosphate (Pi) in the cytosol. The limited availability of Pi in the cytosol restricts the export of triose-phosphates from the chloroplasts via the triose-phosphate:Pi translocator, leading to a rise in 3-phosphoglycerate (3PGA) and a fall in Pi in the stroma. These reciprocal changes in the allosteric activator (3PGA) and the inhibitor (Pi) of ADP-glucose pyrophosphorylase (AGPase) strongly activate the enzyme (Preiss, 1988), increasing the production of ADP-glucose (ADPG) and the synthesis of starch.

The overflow model is supported by various studies on wild-type and mutant plants (Neuhaus et al., 1989, 1990; Neuhaus and Stitt, 1990; Stitt and Sonnewald, 1995; Scott et al., 2000; Strand et al., 2000, Stitt et al., 2010). However, there is good evidence that other mechanisms also contribute to the control of starch synthesis. For example, many species, including Arabidopsis, increase their rate of starch synthesis when shifted from long to short days, so despite the shorter period of photosynthesis, the plants still accumulate sufficient starch during the day to last through the longer night ahead (Chatterton and Silvius, 1980; Gibon et al., 2004). The circadian clock is potentially involved in this anticipatory response, providing information about the expected length of the coming night so that the plant can set an appropriate rate of starch synthesis (Smith and Stitt, 2007; Stitt et al., 2007; Stitt and Zeeman, 2012).

Another mechanism that is potentially important for controlling starch synthesis is the redox regulation of AGPase (Fu et al., 1998; Ballicora et al., 2000; Tiessen et al., 2002). In the light, or in response to high sugar levels in the leaves, AGPase is activated by reduction of an intermolecular disulfide bridge between Cys residues (Cys-81 in Arabidopsis) in the two small subunits of the heterotetrameric holoenzyme (Hendriks et al., 2003; Hädrich et al., 2012). Light-dependent activation and sugar-dependent activation appear to be mediated by the ferredoxin-thioredoxin system and NADP-thioredoxin reductase C, respectively (Michalska et al., 2009; de Dios Barajas-López et al., 2012). Kolbe et al. (2005) found that there was little or no change in the redox status of AGPase when isolated pea (*Pisum sativum*) chloroplasts were incubated in the dark with dithiothreitol (DTT) and Suc, whereas incubation with DTT and 0.1 to 1.0 mM Tre6P led to substantial reduction of the enzyme.

Tre6P is the intermediate of trehalose synthesis; it is synthesized by trehalose-phosphate synthase (TPS) and dephosphorylated to trehalose by trehalose-phosphate phosphatase. Constitutive overexpression of the *Escherichia coli* TPS (otsA) in Arabidopsis gave rise to stunted, early-flowering plants that accumulated more starch in their leaves than wild-type plants (Schluepmann et al., 2003; Kolbe et al., 2005; Wingler et al., 2012). Together, these observations raised the possibility that Tre6P acts as an intermediary in the sugar-induced activation of AGPase. Lunn et al. (2006) found that the amount of Tre6P in Arabidopsis rosettes changes in parallel with diurnal fluctuations in Suc content and the redox status of AGPase, lending correlative support to this hypothesis. However, a direct causal relationship between changes in Suc, Tre6P, and the redox status of AGPase in vivo remains to be demonstrated.

With the onset of darkness, the transitory starch reserves must be managed prudently if they are to last through the night. The pathway of starch degradation in Arabidopsis leaves has been largely resolved, mainly by studies of *starch excess* mutants that fail to degrade their starch effectively during the night (for review, see Zeeman et al., 2010). The initial step involves a cycle of glucan phosphorylation and dephosphorylation to open up the crystalline structure at the surface of the starch granule (Edner et al., 2007; Hejazi et al., 2008; Blennow and Engelsen, 2010). Glc residues within the glucan chains are phosphorylated in the C6 and C3 positions by glucan, water dikinase (GWD) and phosphoglucan, water dikinase (PWD), respectively (Blennow et al., 2002; Ritte et al., 2002, 2006; Baunsgaard et al., 2005; Kötting et al., 2005). Dephosphorylation is catalyzed by the STARCH EXCESS4 (SEX4) and LIKE STARCH EXCESS FOUR2 (LSF2) phosphoglucan phosphatases (Kötting et al., 2009, 2010; Comparot-Moss et al., 2010; Hejazi et al., 2010; Tagliabracci and Roach, 2010; Santelia et al., 2011). Transitory starch is degraded by a combination of β-amylases (principally BAM1 and BAM3; Fulton et al., 2008) and debranching enzymes (Streb et al., 2012) in conjunction with the plastidial disproportionating enzyme (DPE1). The main products are maltose and Glc, which are exported from the chloroplast via the MALTOSE EXCESS1 (MEX1) transporter and the plastidial Glc transporter, respectively (Weber et al., 2000; Niittylä et al., 2004; Weise et al., 2006; Cho et al., 2011). In the cytosol, maltose is metabolized by the cytosolic disproportionating enzyme (DPE2), which catalyzes the reversible transfer of one glucosyl moiety to a soluble heteroglycan, releasing the other as free Glc, which is phosphorylated by hexokinase (Chia et al., 2004; Lu and Sharkey, 2004; Fettke et al., 2005, 2006, 2009). Cytosolic phosphorylase (PHS2) is thought to catalyze the Pi-dependent transfer of terminal glucosyl moieties from the soluble heteroglycan to form glucose-1-phosphate, which enters the cytosolic hexose-phosphate pool, making it available for Suc synthesis, respiration, and other pathways (Fettke et al., 2004, 2005).

In Arabidopsis leaves, starch is degraded in a near-linear manner throughout the night and is almost but not totally exhausted at dawn. The rate of starch degradation is regulated by the circadian clock, which presumably provides information about the expected length of the night (Lu et al., 2005; Graf et al., 2010;

Graf and Smith, 2011; Yazdanbakhsh et al., 2011; Stitt and Zeeman, 2012). This is integrated with information about how much starch has been accumulated during the day, enabling the plant to set an appropriate rate of degradation (Scialdone et al., 2013). The underlying signaling pathways still need to be elucidated. The transcripts of genes involved in starch degradation show large, coordinated diurnal changes (Smith et al., 2004; Lu et al., 2005; Usadel et al., 2008), but at present there is no evidence that these lead to large changes in the levels of the encoded proteins (Smith et al., 2004). Several proteins involved in starch degradation are subject to redox modification, but the physiological significance of this is uncertain (Valerio et al., 2011; Glaring et al., 2012), and as yet there is no evidence of any connection with the control of starch degradation by the circadian clock.

There is also evidence that high levels of Suc in the leaves at night might inhibit starch degradation. When Arabidopsis plants were grown in elevated CO_2, they accumulated higher levels of Suc and starch during the day than control plants in ambient CO_2 and did not start degrading their starch until several hours into the night, when Suc levels had begun to fall (Cheng et al., 1998). Other observations point to a potential role of trehalose metabolism in the regulation of starch turnover. The growth of wild-type Arabidopsis seedlings on trehalose-containing medium without Suc led to the hyperaccumulation of starch in the cotyledons and inhibition of root growth (Wingler et al., 2000; Ramon et al., 2007). The expression of the *APL3* gene, encoding one of the large subunits of AGPase, was induced by trehalose, whereas *SEX1* (encoding GWD) and *BAM3* were repressed.

The level of Tre6P in plant tissues fluctuates in parallel with endogenous changes in Suc content and in response to exogenously supplied Suc, leading to the proposal that Tre6P acts as a signal of Suc availability in plants (Lunn et al., 2006). This strong correlation between Tre6P and Suc has made it difficult to resolve which of the regulatory functions of Suc are mediated by Tre6P and which are not. Therefore, we engineered Arabidopsis plants to express the *E. coli otsA* (*TPS*) gene under the control of an ethanol-inducible promoter, enabling us to bring about short-term changes in the level of Tre6P that are not driven by changes in Suc. These plants were used to test in vivo the hypothesis that Tre6P mediates Suc-linked changes in the rate of starch synthesis via the redox regulation of AGPase (Kolbe et al., 2005) and to investigate the effect of Tre6P on the remobilization of leaf starch reserves. We also investigated how Tre6P might interact with the regulation of starch breakdown by the circadian clock.

RESULTS

Ethanol-Inducible Expression of the *E. coli* TPS in Arabidopsis

Arabidopsis (accession Columbia-0 [Col-0]) was transformed with a construct containing the *E. coli otsA* gene (encoding TPS) under the control of the *Aspergillus nidulans* AlcR/AlcA ethanol-inducible promoter system (Caddick et al., 1998). Primary transformants were selected on kanamycin and then screened by immunoblotting using antibodies against the *E. coli* otsA protein. Plants induced by spraying with 2% (v/v) ethanol contained an immunoreactive protein of the expected size (53 kD) of the *E. coli* otsA (Supplemental Fig. S1). No expression of the protein was detected in wild-type or noninduced plants. After selfing, the T2 and T3 progeny were screened to select two independent homozygous lines, TPS29.2 and TPS31.3 (for details, see "Materials and Methods"). Based on kanamycin resistant:kanamycin sensitive segregation ratios in the T2 generation, these lines each possessed a single transgenic locus (data not shown). In addition, one homozygous line (AlcR) was established that contained the *35S*::*AlcR*::*t-nos* gene construct and the *pAlcA*::*t-ocs* promoter-terminator cassette with no insert, for use as a negative control.

Temporal Kinetics of Starch Accumulation in Response to Induced Overexpression of TPS

The AlcR and TPS29.2 lines were grown under 12-h photoperiod conditions and sampled at 1- to 2-h intervals throughout the light period after spraying the plants with water (noninduced controls) or ethanol (induced). The results are shown in Figure 1, with asterisks indicating time points where the induced TPS29.2 samples were significantly different from all three controls (i.e. AlcR plants sprayed with ethanol or water and TPS29.2 plants sprayed with water) using one-way ANOVA (Holm-Sidak test).

The Tre6P content of the induced TPS29.2 plants was significantly higher than in the noninduced and AlcR control plants by 6 h after induction (Fig. 1A) and continued to increase up to the end of the day (ED), when levels were comparable to those in two similar experiments (Fig. 1A; Supplemental Fig. S2, A and B). The rate of starch accumulation in the induced TPS29.2 plants was the same as in the controls up to 6 h after induction, significantly higher between 6 and 8 h, and then comparable with the controls thereafter (Fig. 1B). The Suc content of the induced TPS29.2 plants was similar to the control plants throughout the day (Fig. 1C). The starch-Suc ratio in the induced TPS29.2 plants was significantly higher than in the controls at 4 and 12 h after induction and also tended to be higher at the intervening time points (Fig. 1D). Glc, Fru, glucose-6-phosphate (Glc6P), and sucrose-6′-phosphate (Suc6P) tended to be lower in the induced TPS29.2 plants in the first hours after induction, but the differences were mostly small and statistically significant only for Fru at 2 h and for Suc6P at 4 h after induction (Supplemental Fig. S3, C–F). The Tre6P-Suc ratio was remarkably similar in all of the control plants and fairly stable throughout the day. The ratio in the induced TPS29.2 plants was significantly higher than in the controls by 4 h after induction, continuing to rise

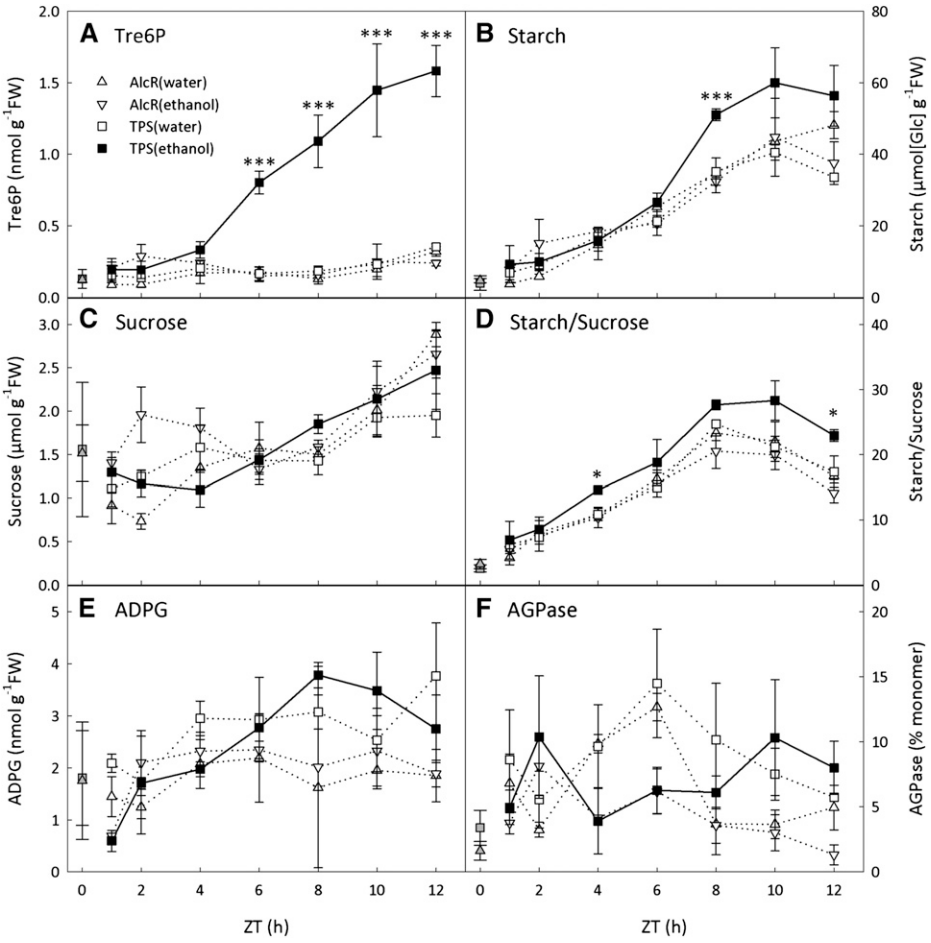

Figure 1. Effect of TPS overexpression on metabolites and the redox status of AGPase in Arabidopsis rosettes during the day. Ethanol-inducible TPS line 29.2 (TPS) and plants expressing the ethanol-binding transcription factor (AlcR) were grown in soil with a 12-h photoperiod. Four-week-old plants were sprayed with water or 2% (v/v) ethanol at the beginning of the day and harvested at 1- or 2-h intervals after spraying for the determination of Tre6P (A), starch (B), Suc (C), the starch-Suc ratio (D), ADPG (E), and the redox status of AGPase (F). Gray symbols at 0 h represent unsprayed AlcR (gray triangles) or TPS (gray squares) plants. Data are means ± SD ($n = 3$). Significant differences (one-way ANOVA, Holm-Sidak test) between the ethanol-sprayed TPS line and the three controls, AlcR (sprayed with water or ethanol) and TPS (water), are indicated by asterisks: $^{*}P < 0.05$ and $^{***}P < 0.001$. FW, Fresh weight; ZT, Zeitgeber time.

up to 6 h, but then changing relatively little during the second half of the day (Supplemental Fig. S3B).

The redox status of AGPase was determined by immunoblotting after SDS-PAGE of leaf proteins under nonreducing conditions, which separates the reduced form of the APS1 small subunit protein (50-kD monomer) from the oxidized form (100-kD dimer). There were no striking differences in either the redox status of AGPase or the ADPG content of the induced TPS29.2 plants compared with the controls, with the values from the former overlapping with at least one of the controls at any given time point (Fig. 1, E and F). Retention of reduced APS1 protein during extraction and analysis was confirmed by including leaf extracts from wild-type Col-0 and the *pgm* mutant on each gel (Supplemental Fig. S4). On average, the percentage of APS1 protein present as the 50-kD monomer was 10 times higher in the *pgm* samples than in the wild type, comparable to the previously reported differences between these genotypes (Lunn et al., 2006).

In two further experiments, TPS29.2, TPS31.3, wild-type Col-0, and AlcR plants were sprayed with water or 2% (v/v) ethanol at the beginning of the day and harvested 12 h later, at the ED. In both experiments, the wild-type (0.17–0.37 nmol g^{-1} fresh weight) and AlcR (0.18–0.39 nmol g^{-1} fresh weight) rosettes contained very similar amounts of Tre6P, with no significant differences between the two genotypes or between water and ethanol-sprayed plants (Supplemental Fig. S2, A and B). Induced TPS29.2 and TPS31.3 plants had much higher Tre6P (1.44–2.21 nmol g^{-1} fresh weight), representing a 4- to 11-fold increase over the respective noninduced plants and control genotypes. There was no significant effect of induced overexpression of TPS on the Suc or trehalose contents of the plants (Supplemental Fig. S2, C, D, and I) and only small changes in hexose sugars (Supplemental Fig. S2, J–M). Ethanol spraying slightly decreased the amount of starch accumulated by wild-type plants by the ED and, in one experiment, increased ED starch content by about 50% in the TPS31.3 line (Supplemental Fig. S2, E and F). There were only small and mostly nonsignificant differences in the AlcR and TPS29.2 plants. Compared with the respective water-sprayed controls, the starch-Suc ratio at the ED was slightly decreased in the wild-type plants ($P < 0.01$) after ethanol treatment, unaffected in the AlcR plants, and 22% to 72% higher in the two TPS lines (Supplemental Fig. S2, N and O). The percentage of APS1 protein in the 50-kD monomeric form was not significantly affected by ethanol spraying except for a

decrease in the AlcR line in one experiment (Supplemental Fig. S2, G and H).

In summary, induction of TPS expression consistently increased Tre6P levels in the independent TPS lines, TPS29.2 and TPS31.3. There was a small but consistent increase in the starch-Suc ratio in the induced TPS plants but no reproducible effect on the redox status of AGPase or the starch content on its own.

Tobacco (*Nicotiana tabacum*) plants with constitutively elevated levels of Tre6P were reported to have higher rates of photosynthesis per unit leaf area than wild-type plants (Pellny et al., 2004). To test if a short-term rise in Tre6P could affect photosynthetic capacity, we measured net CO_2 assimilation rates in TPS29.2 and AlcR plants 12 h after spraying with water or 2% (v/v) ethanol. Induction of TPS expression had no obvious effect on photosynthetic CO_2 fixation in the TPS29.2 plants when rates were compared with those in unsprayed or water-sprayed plants or in AlcR control plants (Supplemental Fig. S5).

Inhibition of Starch Degradation in Arabidopsis Leaves with High Tre6P at Night

We next investigated whether Tre6P has any influence on starch remobilization in Arabidopsis leaves at night. Wild-type, AlcR, TPS29.2, and TPS31.3 plants were grown in soil with a 12-h photoperiod, in parallel with the plants described in Supplemental Figure S2 (experiment 1). The plants were sprayed with water or 2% (v/v) ethanol at the beginning of the night and harvested 12 h later, at the end of the night (EN), for metabolite and enzyme analysis.

Induction of TPS expression in the TPS29.2 and TPS31.3 plants led to a 2- to 3-fold increase in Tre6P compared with control plants, reaching levels (0.46–0.51 nmol g^{-1} fresh weight; Fig. 2A) that were slightly higher than those seen in wild-type plants at the ED (Supplemental Fig. S2, A and B). There were no significant changes in trehalose content in the TPS29.2 or TPS31.3 plants after induction (Fig. 2B). There was a small but significant increase in Suc in wild-type plants after ethanol spraying, whereas Suc fell slightly in all the other genotypes, with the decrease being significant in TPS29.2 and TPS31.3 ($P < 0.05$; Fig. 2C). Ethanol treatment led to a significant increase in Glc in wild-type and AlcR plants but no change in the TPS lines (Fig. 2D), whereas Fru fell slightly in wild-type, AlcR, and TPS29.2 plants ($P < 0.05$) but not in TPS31.3 (Fig. 2E).

The wild-type and AlcR plants contained only a small residue of starch (5.4–8.5 μmol [Glc] g^{-1} fresh weight) at the EN. In the parallel daytime induction experiment (Supplemental Fig. S2E), wild-type, AlcR, and TPS control plants sprayed with water accumulated 62 to 79 μmol [Glc] g^{-1} fresh weight of starch by the ED. This comparison reveals that the wild-type and AlcR plants had degraded most, but not quite all, of their starch during the night (Fig. 2F), which is typical for Arabidopsis plants grown in a 12-h photoperiod (Gibon et al., 2004; Smith and Stitt, 2007; Hädrich et al., 2012). There was no obvious effect of ethanol on EN starch content in either of the control lines. In contrast, the induced TPS29.2 and TPS31.3 plants contained a much greater residual amount of starch at the EN (34–36 μmol [Glc] g^{-1} fresh weight), indicating that they had degraded only half of their starch reserves (Fig. 2F).

Conceivably, resynthesis of starch from the products of starch degradation could have given the appearance of a lower net rate of starch breakdown in induced TPS29.2 and TPS31.3 plants. However, immunoblotting showed that AGPase was in the fully oxidized (i.e. low-activity) form in all of the plants harvested at the EN, including the induced TPS29.2 and TPS31.3 plants (data not shown). Furthermore, there were no obvious differences in ADPG content between the induced TPS29.2 and TPS31.3 plants at the EN compared with the controls (data not shown). In fact, ADPG was barely detectable (less than 0.02 nmol g^{-1} fresh weight) in any of the dark-harvested plants, in contrast to plants harvested in the light, which contained 0.5 to 4.0 nmol g^{-1} fresh weight ADPG (Fig. 1E). Thus, resynthesis of starch appears unlikely to explain the higher EN starch content of the induced TPS plants.

In Arabidopsis leaves, the main product of starch degradation is maltose, which is exported from the chloroplasts to the cytosol and metabolized further to provide substrates for Suc synthesis and respiration (Niittylä et al., 2004; Weise et al., 2004). Maltose levels were 40% lower in the induced TPS29.2 and TPS31.3 plants than in the mock-induced and other controls, with this decrease being significant in TPS29.1 ($P < 0.05$; Fig. 2G). Maltotriose appeared to be marginally but nonsignificantly decreased in both TPS lines (Fig. 2H).

The sugars produced by starch degradation are used for maintenance respiration and growth. The rate of dark respiration in ethanol-induced TPS29.2 plants was not significantly different from the rates in nonsprayed and water-sprayed controls, and a similar pattern was observed in AlcR control plants (Supplemental Fig. S6). Protein synthesis is essential for growth and represents one of the biggest energy demands for the plant. We used polysome-loading analysis (Piques et al., 2009) as a proxy for assessing the rate of protein synthesis. During the night, the percentage of ribosomes bound to mRNA was slightly lower in ethanol-induced TPS29.2 plants than in water-sprayed (i.e. noninduced) control plants (Supplemental Fig. S7), but the differences were not statistically significant.

These results showed that elevated levels of Tre6P led to substantial inhibition of starch degradation in Arabidopsis leaves at night. To better understand the effects of Tre6P on starch breakdown, we performed a series of time-course experiments with the inducible TPS lines, comparing the nocturnal changes in Tre6P, starch, and sugars in induced versus noninduced plants.

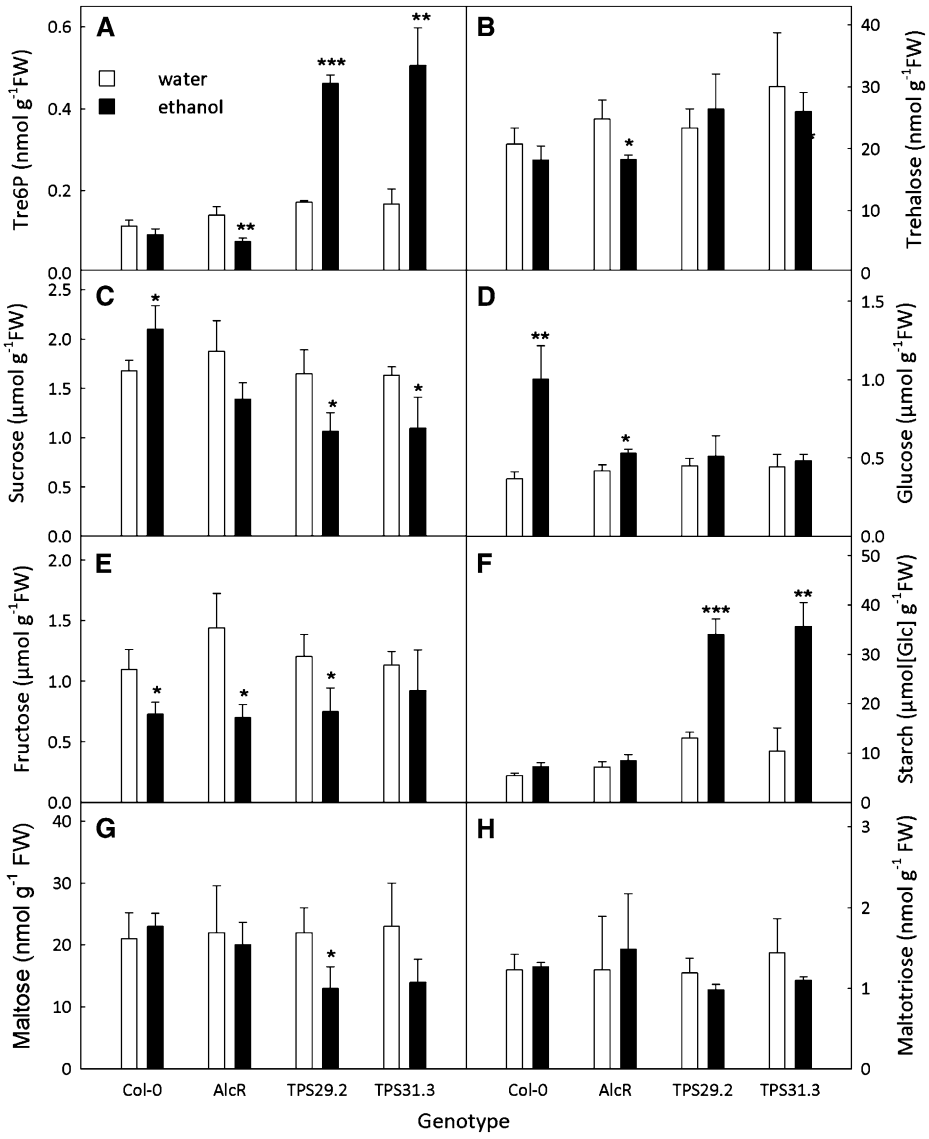

Figure 2. Induced changes in the Tre6P content of Arabidopsis rosettes at night. Ethanol-inducible TPS plants (TPS29.2 and TPS31.3) were grown in soil with a 12-h photoperiod. Wild-type plants (Col-0) and plants expressing the AlcR ethanol-binding transcription factor (AlcR) were grown as controls. Four-week-old plants were sprayed with water (white bars) or 2% (v/v) ethanol (black bars) at the beginning of the night. Pools of 10 rosettes were harvested 12 h later at the EN for the determination of Tre6P (A), trehalose (B), Suc (C), Glc (D), Fru (E), starch (F), maltose (G), and maltotriose (H). Data are means ± SD ($n = 3$). Significant difference between ethanol- and water-treated plants from the same genotype are indicated by asterisks (Student's t test): $^{*}P < 0.05$, $^{**}P < 0.01$, and $^{***}P < 0.001$. FW, Fresh weight.

Temporal Kinetics of Induced Changes in Tre6P, Starch, and Sugar Levels in the Dark

TPS29.2 and TPS31.3 plants were grown in soil with a 12-h photoperiod and sprayed with either water or 2% (v/v) ethanol at the ED. Triplicate pools of five plants were harvested in the light before spraying (ED) and at 2- or 4-h intervals during the night for metabolite analysis. The nocturnal changes in metabolites were qualitatively similar in both of the inducible TPS lines; therefore, for brevity, results are shown only for line TPS29.2 (Fig. 3, A–D).

With the onset of darkness, Tre6P fell in the non-induced plants, then began to rise after 2 h in the dark, but remained lower than the levels seen at the ED (Fig. 3A). The initial fall in Tre6P was less pronounced in the induced plants, and by 2 h, the induced plants contained significantly more Tre6P than the controls. Within 4 h of induction, Tre6P exceeded the level at the ED, rising even further later in the night. These results suggest that within 2 h of induction, expression of the heterologous TPS might already be counteracting the fall in Tre6P levels seen in the first hours of the night.

In the noninduced plants, starch levels decreased at a more or less constant rate throughout the night, and by the EN, the plants had remobilized almost 90% of their starch reserves (Fig. 3B). This resembles the pattern seen in wild-type plants in many previous experiments (Smith and Stitt, 2007; Graf et al., 2010; Pyl et al., 2012). Although the initial rate of starch degradation was similar in the ethanol-sprayed plants, it slowed down considerably from about 2 h after induction, and at the EN, the plants retained about 30% of their original starch reserves.

In the noninduced plants, Suc levels from 2 to 6 h into the night were about 20% lower than at the ED, and they fell slightly further toward the EN (Fig. 3C).

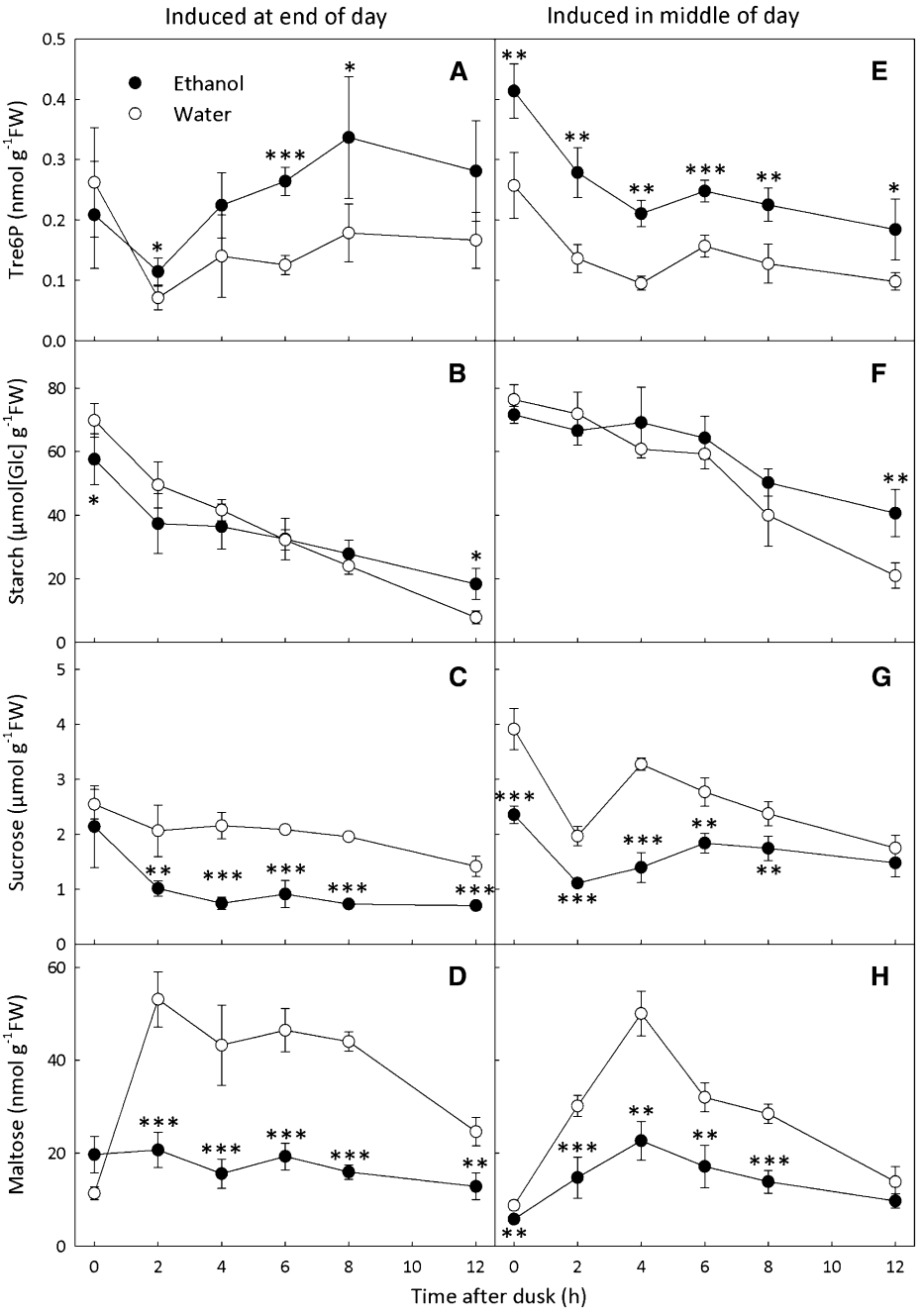

Figure 3. Inhibition of starch degradation at night by induced high levels of Tre6P. Ethanol-inducible TPS29.2 plants were grown in soil with a 12-h photoperiod. Four-week-old plants were sprayed with water (white circles) or 2% (v/v) ethanol (black circles) at the ED (A–D) or in the middle of the day (E–H). Pools of five rosettes were harvested at the ED and at 2- or 4-h intervals through the night for the determination of Tre6P (A and E), starch (B and F), Suc (C and G), and maltose (D and H). Data are means ± SD ($n = 3$). Significant differences between the water- and ethanol-treated plants at the same time point are indicated by asterisks (Student's t test): $^{*}P < 0.05$, $^{**}P < 0.01$, and $^{***}P < 0.001$. FW, Fresh weight.

At all time points in the dark, the induced plants had less Suc than the noninduced plants at the EN (Fig. 3C). Glc decreased markedly at the beginning of the night in noninduced plants and fell even further (27%–43%) in the induced plants (Supplemental Fig. S8A). Fru was also 25% to 46% lower in the induced plants (Supplemental Fig. S8B). Glc6P, fructose-6-phosphate (Fru6P), and Suc6P were all lower in the induced plants compared with the noninduced controls (Supplemental Fig. S8, C–E). Maltose was low in the noninduced plants at the ED, increased over 4-fold during the first 2 h of darkness, and stayed more or less constant for the next 6 h before falling back again by the EN (Fig. 3D). In sharp contrast, maltose remained low throughout the night in the induced plants. These plants also had less maltotriose than the noninduced controls (Supplemental Fig. S8F).

A second time-course experiment was carried out to investigate if starch breakdown was even more strongly inhibited if Tre6P levels were already elevated at the beginning of the night. Plants were sprayed with either water or ethanol in the middle of the day (i.e. 6 h before the ED), and rosettes were harvested at the ED and at 2- or 4-h intervals during the night. At the ED

and at each time point through the night, Tre6P levels were about 2-fold higher in the induced plants than the noninduced controls (Fig. 3E). In both sets of plants, Tre6P fell by about half over the first 4 h of darkness, showed a slight rise at 6 h, but then fell back again toward the EN.

Starch decreased in a fairly linear manner throughout the night in the noninduced plants, and by the EN, nearly 80% of the ED starch reserves had been remobilized (Fig. 3F). In the induced plants, which started the night with elevated levels of Tre6P, there appeared to be little loss of starch during the first half of the night, as the plants retained almost 90% of their ED starch content after 6 h in the dark. The rate of starch degradation appeared to accelerate to some extent during the second half of the night. However, by the EN, the plants still retained over 50% of their ED starch, which was twice as much as the noninduced controls. The acceleration of starch degradation in the second half of the night, while Tre6P levels stayed fairly constant, suggested that the inhibitory effect of high Tre6P on starch breakdown had been partially overridden in some way. With the exception of Fru and Fru6P, the induced and noninduced plants showed qualitatively similar differences to those in the ED induction experiment, with the induced plants having lower Suc and maltose levels (Fig. 3, G and H) as well as less Glc, Glc6P, Suc6P, and maltotriose (Supplemental Fig. S9, A, C, E, and F). Fru was not significantly affected in the induced plants, and Fru6P only decreased toward the EN (Supplemental Fig. S9, B and D).

To summarize, in both time-course experiments the noninduced control plants showed fairly similar behavior: (1) the rate of starch degradation was more or less constant throughout the night, and by the EN, most of the starch had been degraded; (2) maltose was low at the ED and rose as the plants started to degrade their starch; and (3) Suc levels dropped when the lights went out, but during the middle hours of the night, they tended to start rising again or at least stabilize. In comparison, the induced plants degraded less of their starch during the night, their maltose content increased to a much lesser extent or did not increase at all, they contained less maltotriose, and there was a weaker recovery in Suc levels after the initial fall at the beginning of the night.

How Does Tre6P Affect Starch Degradation?

Arabidopsis mutants that lack the capacity to export maltose from the chloroplasts (*mex1*) or metabolize it in the cytosol (*dpe2*) accumulate high levels of maltose (Chia et al., 2004; Lu and Sharkey, 2004; Niittylä et al., 2004). As the induced TPS plants had less maltose than the noninduced controls (Figs. 2G and 3, D and H), this suggested that neither maltose export nor its metabolism in the cytosol was restricted in the induced TPS plants. Therefore, to investigate potential targets for Tre6P inhibition, we focused our attention mainly on upstream steps in the pathway of starch breakdown in the chloroplasts.

Immunoblotting of leaf extracts from AlcR, TPS29.2, and TPS31.3 plants showed no obvious differences in GWD, PWD, or SEX4 protein abundance in ethanol- versus water-sprayed plants (Supplemental Figs. S10, A and B, and S11). Native PAGE, followed by in-gel activity staining, indicated that the maximal activities of the plastidial phosphorylase (PHS1), cytosolic phosphorylase (PHS2), and DPE2 were very similar in leaf extracts from AlcR, TPS29.1, and TPS31.3 plants, irrespective of whether the plants were sprayed with water or ethanol (Supplemental Fig. S10, C and D). From these results, we have no evidence of Tre6P-induced changes in the maximal activities or protein abundances of the main enzymes involved in starch phosphorylation and dephosphorylation (GWD, PWD, and SEX4), the minor pathway of starch degradation via starch phosphorylase (PHS1), or the cytosolic pathway of maltose catabolism (DPE2 and PHS2).

We compared the structures and properties of starch granules from induced and noninduced TPS29.2 plants to seek clues to the mechanism of inhibition of starch degradation in plants with elevated Tre6P. TPS29.2 plants were grown with a 12-h photoperiod, sprayed with either water or ethanol in the middle of the day, and harvested at 2-h intervals starting from the ED. Starch granules were isolated from both sets of plants and examined with a scanning electron microscope. The granules from both induced and noninduced plants appeared to be similar in size and general shape (Supplemental Fig. S12, A and B), having the flat discoid structure that is typical of Arabidopsis leaf starch (Zeeman et al., 2002). However, the granules from the induced TPS plants harvested during the night, particularly at 2 and 4 h, appeared to have a more uneven surface than those from the noninduced plants (Supplemental Fig. S12, C–J).

The C6-phosphate content of the granules was determined by gentle acidic hydrolysis of the α-1,4- and α-1,6-glucosidic bonds, releasing the individual Glc moieties from the glucan chains, followed by enzymatic measurement of Glc6P and Glc (Haebel et al., 2008). Total phosphate content of the starch granules, reflecting both C6 and C3 phosphorylation, was measured colorimetrically after acidic hydrolysis of the starch and treatment with alkaline phosphatase. Large numbers of plants were needed to isolate enough starch granules for these measurements, and due to growth space limitations, only single determinations were possible for each time point. The results of two independent experiments are presented separately (Fig. 4). Tre6P was measured in replicate plants harvested in parallel with the samples for starch granule isolation and was substantially higher in the induced plants compared with the noninduced controls (Fig. 4, A and B). In both experiments, the C6-phosphate content tended to decrease during the night in starch granules from noninduced plants but remained fairly

constant in the granules from the induced TPS plants (Fig. 4, C and D). The total phosphate content of the starch granules showed a similar pattern, generally decreasing through the night in the noninduced control plants but remaining more or less constant in the induced plants with elevated Tre6P (Fig. 4, E and F).

We investigated the ability of recombinant potato (*Solanum tuberosum*) GWD and Arabidopsis PWD to phosphorylate starch granules isolated from induced and noninduced TPS29.2 plants. Phosphorylation was determined by measuring the incorporation of radioactivity upon the incubation of isolated starch granules with the enzymes and [β-^{33}P]ATP. Again, due to the large number of plants needed to isolate starch granules, only single measurements were possible at each time point, so the experiment was done twice and the results of each experiment are presented separately (Fig. 4, G and H). While there were some differences between the two experiments, the following trends were observed in both experiments. The amount of ^{33}P incorporated into the starch granules varied with the time of harvest of the plants, with little phosphorylation occurring with starch granules isolated from leaves harvested at the ED and more rapid phosphorylation at later times. In all of the samples harvested in the dark, less ^{33}P was incorporated into the granules from induced plants than those from noninduced controls.

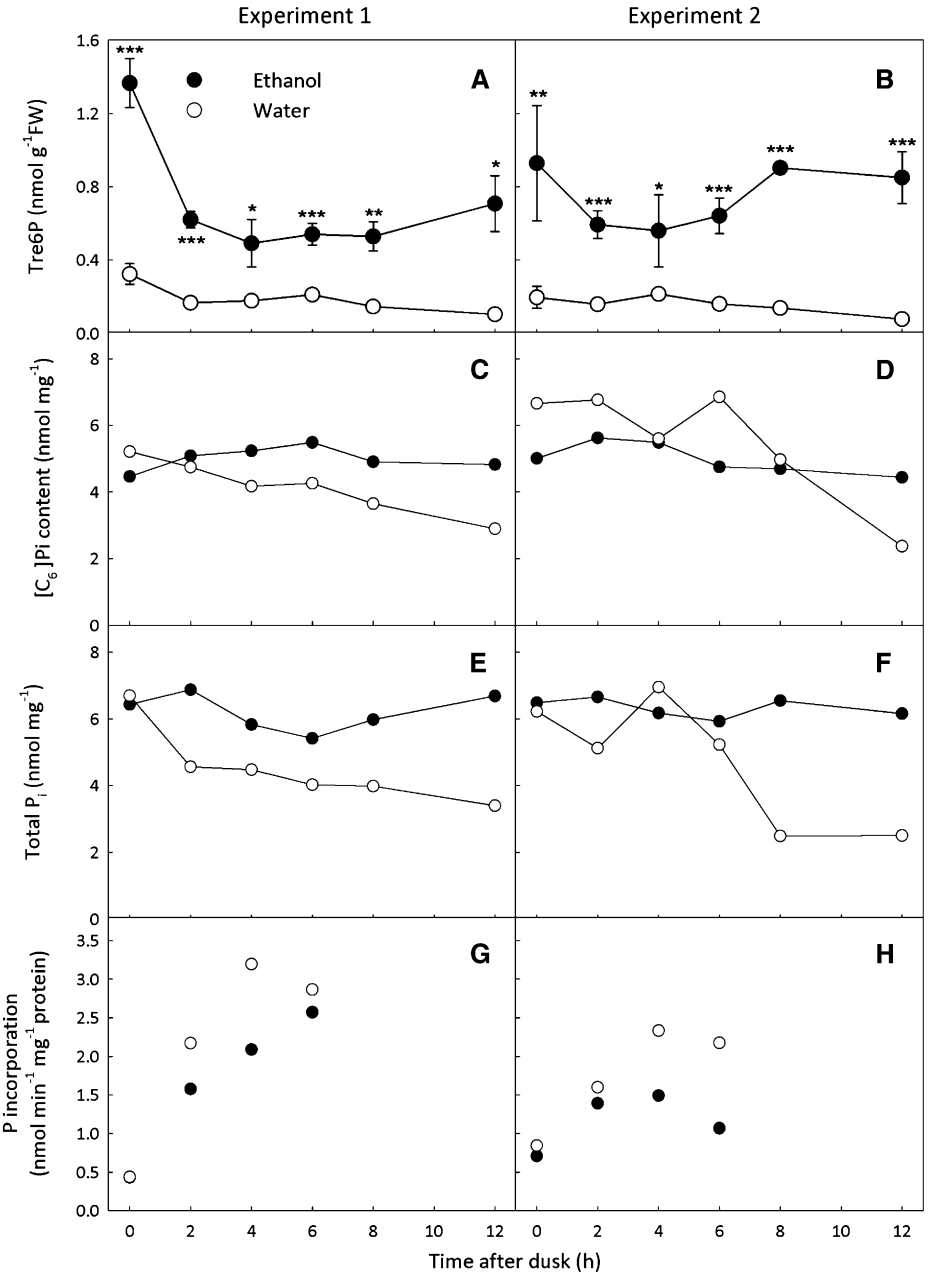

Figure 4. Phosphate content and phosphorylation of starch granules isolated from induced and noninduced TPS29.2 plants at night. Inducible TPS29.2 plants were sprayed with water (white circles) or 2% (v/v) ethanol (black circles) 6 h before the ED. A and B, Rosettes were harvested at the ED and at 2 to 12 h into the night for the determination of Tre6P and the isolation of starch granules. C to F, The phosphate content of the starch granules was determined after enzymatic and acid hydrolysis. C and D, Pi content (C_6 only). E and F, Total phosphate content ($C_6 + C_3$). G and H, In vitro phosphorylation of the granules by recombinant potato GWD and Arabidopsis PWD was determined by the incorporation of ^{33}P from [β-^{33}P]ATP. Tre6P data are means ± SD (n = 3 or 4). Significant differences between ethanol- and water-treated plants are indicated by asterisks (Student's t test): $^*P < 0.05$, $^{**}P < 0.01$, and $^{***}P < 0.001$. Starch granule data are single measurements from two independent experiments: experiment 1 (A, C, E, and G) and experiment 2 (B, D, F, and H). FW, Fresh weight.

Together, these results indicate that the induction of TPS affected both the phosphate content of the starch granules and their suitability as substrates for phosphorylation by GWD and PWD. This suggested that the cycle of phosphorylation by GWD and PWD and dephosphorylation by SEX4 phosphoglucan phosphatase (supplemented by LSF2) might be perturbed in plants with high nighttime levels of Tre6P. As no evidence was found of Tre6P-induced changes in the abundance of the GWD, PWD, or SEX4 proteins (Supplemental Figs. S10 and S11), we investigated whether Tre6P or its derivative, trehalose, might act directly as activators or inhibitors of these enzymes.

Does Tre6P or Trehalose Directly Affect the Activities of Enzymes Involved in Starch Degradation?

The effects of Tre6P and trehalose on the activities of starch (de)phosphorylating enzymes were determined by in vitro activity assays of recombinant potato GWD, Arabidopsis PWD, and Arabidopsis SEX4. Neither Tre6P (0.01–1.0 mM) nor trehalose (0.5–1.0 mM) had any consistent inhibitory or activating effect on GWD or SEX4 activity (Supplemental Table S1). The rate of phosphate incorporation by PWD was very low in the controls without Tre6P, and the addition of Tre6P did not affect the activity (data not shown). BAM3 is the main β-amylase isoform responsible for starch hydrolysis in Arabidopsis leaves (Fulton et al., 2008). Recombinant BAM3 activity was assayed colorimetrically in the absence or presence of 0.05 to 1.0 mM Tre6P or trehalose. Tre6P appeared to inhibit BAM3 activity very slightly, but even at the highest concentration tested (1 mM), the activity was only decreased by 12% (Supplemental Table S1). Trehalose had no obvious effect on BAM3 activity.

To summarize, the low maltose levels and altered patterns of starch phosphorylation in the induced TPS plants pointed to inhibition of an early step in the pathway of starch breakdown. However, the immunoblotting and enzyme activity experiments did not reveal any evidence of a direct effect of Tre6P on the enzymes involved in those steps, leaving open the possibility that Tre6P acts indirectly, and not necessarily within the chloroplasts, to inhibit starch degradation. Therefore, it was of interest to investigate whether Tre6P is even present in the chloroplasts.

Subcellular Compartmentation of Tre6P

We used nonaqueous density gradient fractionation (Gerhardt and Heldt, 1984; Stitt et al., 1989) to determine the subcellular compartmentation of Tre6P in wild-type Arabidopsis plants. This technique allows the chloroplastic and vacuolar pools of metabolites to be resolved from the rest of the cell, which is mostly composed of the cytosol but also includes the mitochondria and peroxisomes.

Wild-type Arabidopsis plants were grown in either short-day (8 h of light/16 h of dark) or equinoctial (12 h of light/12 h of dark) conditions. In both experiments, rosettes were harvested from 5-week-old plants around 4 h before the ED, and the leaf material was fractionated on three separate nonaqueous gradients (i.e. three technical replicates). The subcellular compartmentation of Tre6P was found to be similar in both sets of plants. Based on the distribution of marker enzymes for chloroplasts, cytosol, and vacuole, it was estimated that 16% to 22% of the Tre6P was in the chloroplasts, 7% to 11% was in the vacuoles, and 71% to 72% was elsewhere, presumably mostly in the cytosol (Table I).

As a cross check, we compared the distribution of Tre6P with metabolite markers for the three compartments. Suc6P, which is a cytosolic marker (MacRae and Lunn, 2006), showed an almost identical distribution to Tre6P across all three gradients from the short-day grown plants, with a Pearson's correlation coefficient (r) of 0.981 (Supplemental Fig. S13A). Based on the distribution of marker enzymes, Suc6P was assigned predominantly (66%–72%) but not exclusively to the cytosol in both experiments, although there was considerable variation between aliquots from the 12-h-grown plants (Table I). Tre6P was less well correlated (r = 0.843; Supplemental Fig. S13B) with ribulose-1,5-bisphosphate (RuBP), a chloroplast metabolite marker (Raines, 2003), which was found to be almost exclusively in the chloroplasts (Table I). Tre6P was poorly correlated with nitrate (r = 0.363; Supplemental Fig. S13C), which is considered to be a vacuolar marker (Krueger et al., 2009).

The in vivo concentration of Tre6P in each compartment was estimated from the total Tre6P content of the leaf, its distribution between the chloroplasts, cytosol, and vacuole, and the likely volumes of these compartments. In Arabidopsis leaves, starch is found predominantly in the palisade and spongy mesophyll cells. Therefore, to estimate the maximal in vivo concentrations likely to be found in these starch-containing cells, it was assumed that all of the Tre6P in the leaf was present in the mesophyll cells. In Arabidopsis, the palisade and mesophyll cells together represent between 72% and 89% of the total leaf thickness (Wuyts et al., 2010), which is considered to be a reasonable proxy for the cell volume expressed as a percentage of the total leaf volume. However, these leaf thickness measurements do not take into account the contributions of the vascular tissue and intracellular air spaces to the total leaf volume, with the latter in particular likely to represent a substantial fraction of the total. Unpublished data (H. Poorter and F.Z.J., Jülich, personal communication) indicate that the mesophyll cells occupy 65% to 76% of the total leaf volume in Arabidopsis, with a mean value of 69%. We used this mean value in our calculations of the in vivo concentrations of Tre6P. Due to the lack of suitable estimates for subcellular volumes in Arabidopsis leaves, we used the percentages of total leaf volume reported for spinach (*Spinacia oleracea*): chloroplasts,

Table I. *Subcellular compartmentation of Tre6P in Arabidopsis rosettes*

Wild-type Arabidopsis Col-0 plants were grown in 8-h-light/16-h-dark (experiment 1) and 12-h-light/12-h-dark (experiment 2) conditions for 5 weeks. In both experiments, rosettes were harvested around 4 h before the end of the light period, rapidly quenched in liquid N_2, ground to a fine powder at −70°C, lyophilized, and then fractionated by centrifugation on three separate nonaqueous density gradients. The amount of Tre6P in the original plant material and in the gradient fractions was measured by LC-MS/MS using enzymatically calibrated standards and a [^{2}H]Tre6P internal standard to correct for ion suppression and matrix effects (Lunn et al., 2006). Suc6P was measured by LC-MS/MS (Lunn et al., 2006) and RuBP by ion-pair reverse-phase LC-MS/MS (Arrivault et al., 2009). The subcellular distribution of each metabolite between chloroplasts, cytosol, and vacuoles was determined by reference to marker enzymes and metabolites for each compartment, using the BESTFIT program (Klie et al., 2011). The in vivo concentrations were estimated assuming that all of the metabolites were in the mesophyll cells and that these cells occupy 69% of the total leaf volume (for details, see text). For each experiment, data represent means ± SD of measurements from three aliquots of the pooled plant material harvested in the individual experiments.

Metabolite	Amount	Subcellular Distribution			Concentration in Vivo		
		Chloroplast	Cytosol	Vacuole	Chloroplast	Cytosol	Vacuole
	nmol g^{-1} fresh wt		*% of total*			*μM*	
Tre6P							
Experiment 1	0.196 ± 0.012	16 ± 11	72 ± 12	11 ± 5	0.18 ± 0.11	3.81 ± 0.76	0.05 ± 0.02
Experiment 2	0.351 ± 0.077	22 ± 9	71 ± 14	7 ± 10	0.46 ± 0.26	6.71 ± 2.02	0.05 ± 0.06
Suc6P							
Experiment 1	0.72 ± 0.03	10 ± 1	72 ± 4	18 ± 4	0.4 ± 0.0	13.9 ± 0.1	0.3 ± 0.1
Experiment 2	1.14 ± 0.21	25 ± 16	66 ± 15	9 ± 4	1.7 ± 1.4	19.8 ± 3.4	0.2 ± 0.1
RuBP							
Experiment 1	45.3 ± 3.1	92 ± 5	6 ± 6	2 ± 2	237 ± 5	76 ± 72	2 ± 2
Experiment 2	60.3 ± 24.3	89 ± 3	5 ± 4	6 ± 2	304 ± 112	91 ± 94	8 ± 3

25.4%; cytosol, 5.4%; and vacuole, 68% (Winter et al., 1994). These seem likely to be a reasonable approximation for Arabidopsis leaves, given that both species are herbaceous, nonsclerophyllous, nonsucculent, C_3 eudicots. Furthermore, values reported for barley (*Hordeum vulgare*; chloroplasts, 27.8%; cytosol, 9.7%; and vacuole, 60.5%; Winter et al., 1993), a more distantly related monocot species, differ by a factor of less than two from the spinach data. The maximal in vivo concentrations of Tre6P in mesophyll cells were estimated to be between 0.18 and 0.46 μM in the chloroplasts, 3.81 and 6.71 μM in the cytosol, and 0.05 μM in the vacuole (Table I).

Responses of Starch Degradation, Maltose Levels, and Tre6P after an Unexpected Early Dusk

Finally, we investigated the relationship between circadian clock- and Tre6P-mediated regulation of starch breakdown. Starch breakdown is under the control of the circadian clock, which acts to prevent premature exhaustion of starch (Lu et al., 2005; Graf et al., 2010; Graf and Smith, 2011; Yazdanbakhsh et al., 2011; Scialdone et al., 2013). If Arabidopsis plants are darkened several hours before the customary dusk, they break down their starch at a slower rate than usual so that their carbohydrate reserves are not exhausted before the expected dawn (Lu et al., 2005; Graf et al., 2010). Given the observed inhibitory effect of Tre6P on the rate of starch breakdown, we investigated if this clock-dependent regulation of starch breakdown is mediated by Tre6P, or if the clock acts independently of Tre6P, or even antagonistically to Tre6P.

Wild-type plants were grown under equinoctial conditions for 3 weeks and harvested through two sequential diurnal cycles: the first being the control (12 h of light/12 h of dark) and the second the early-dusk treatment, with the lights being switched off after 8 h, subjecting the plants to a 16-h night. A dense series of sampling points was included after both light/dark transitions to capture changes occurring during the period when the rate of starch degradation is likely to be set for the night ahead.

During the 12-h/12-h diurnal cycle, the plants accumulated starch in a linear manner through the day and degraded over 95% of their starch reserves during the night (Fig. 5A). The dense series of time points taken shortly after darkening the plants indicates that there may be a lag before net starch degradation begins. Maltose levels were low during the light period but showed a significant rise between 8 h and the end of the light period, rose further but gradually over the first 2 h of the night, remained high until 6 h, and then declined (Fig. 5B). Suc increased in two phases during the 12-h light period, fell abruptly in the first 1 h of the night, and then recovered (Fig. 5C). The gradual rise in maltose and the transient fall in Suc levels provide supporting evidence that there is a delay before the plants begin to degrade their starch after being suddenly darkened (Pal et al., 2013). Tre6P tracked Suc closely during the day and the first 1 h of the night, except that the recovery in Tre6P levels after falling at the beginning of the night was slightly delayed compared with Suc (Fig. 5D). These transient changes were not clearly seen in the experiments shown in Figure 3 because samples were not harvested until 2 h after dusk.

After the early dusk, starch was degraded at about half the rate seen during the preceding 12-h night (Fig. 5A), confirming the results of Graf et al. (2010). The dense time points for the starch (Fig. 5A), the slow

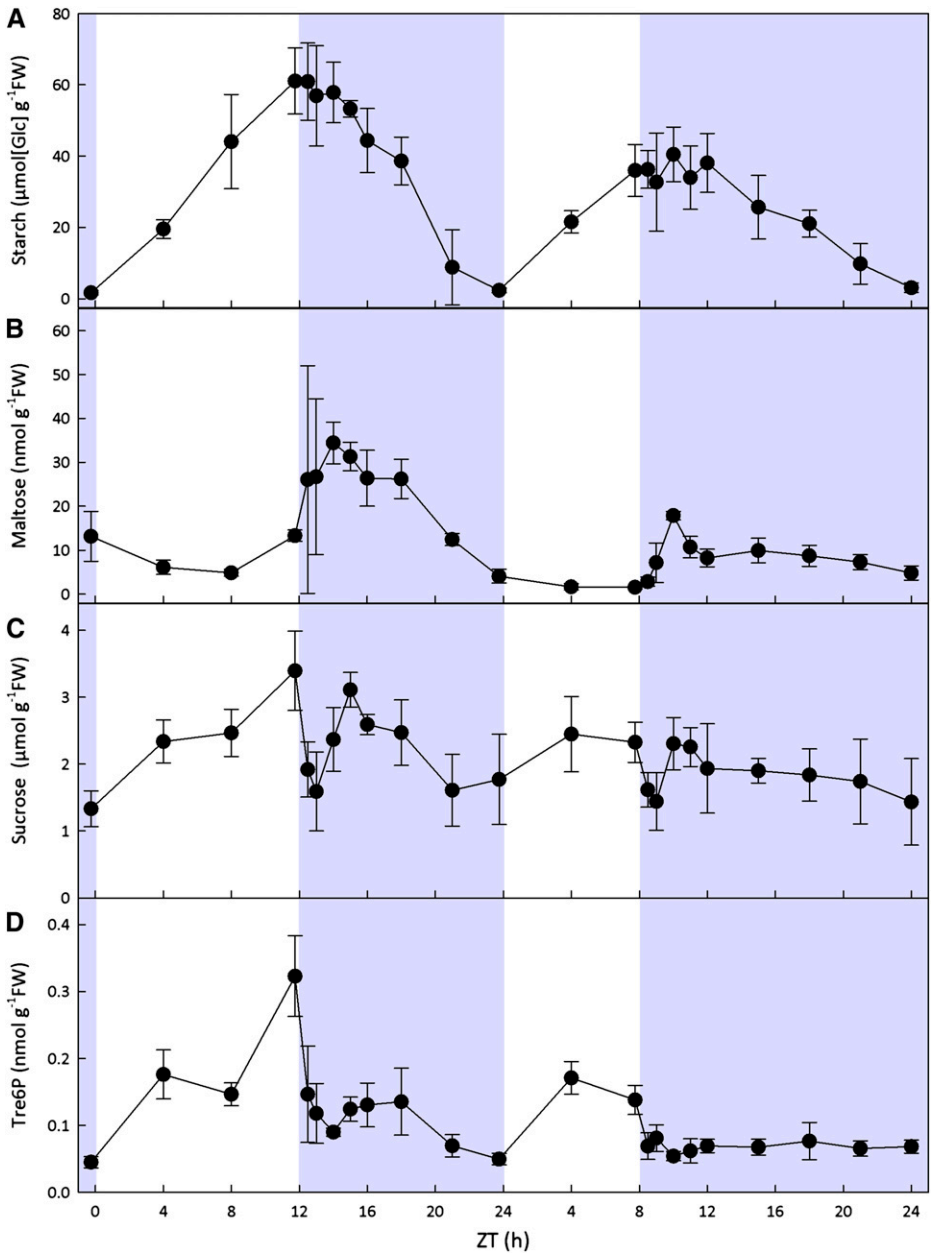

Figure 5. Effect of an early dusk on metabolite levels in Arabidopsis leaves. Wild-type Arabidopsis Col-0 plants were grown in soil with a 12-h photoperiod for 3 weeks. Pools of five rosettes were harvested at various intervals through two sequential diurnal cycles, 12 h of light/12 h of dark (control; 1) and 8 h of light/16 h of dark (early dusk treatment; 2), for the measurement of starch (A), maltose (B), Suc (C), and Tre6P (D). Data are means ± SD (n = 4). FW, Fresh weight; ZT, Zeitgeber time.

increase of maltose (Fig. 5B), and the transient fall in Suc (Fig. 5C) again indicate that there may be a lag before starch degradation begins. After this transient, maltose levels peaked at a noticeably lower level than during the previous 12-h night and fell back more quickly, remaining at a low level throughout the second half of the night (Fig. 5B). Suc was also lower in the 16-h night than in the 12-h night. Tre6P levels fell in the first 30 min of darkness after the early dusk, as seen in the unperturbed light/dark cycle, but then remained low and more or less constant throughout the night (Fig. 5D). It is important to note that the levels of Tre6P in the 16-h night period following the early dusk were lower than in the 12-h night, even though the rate of starch breakdown was approximately 50% lower in the 16-h night than in the 12-h night (Fig. 5A).

Suc6P showed a similar pattern of changes to Suc during both the 12-h/12-h and 8-h/16-h diurnal cycles (Fig. 5C; Supplemental Fig. S14A). ADPG was barely detectable during either the 12-h night or the prolonged 16-h night after the early dusk (Supplemental Fig. S14B).

DISCUSSION

Subcellular Compartmentation and in Vivo Concentrations of Tre6P

In Arabidopsis, TPS1 is the only isoform that has been unequivocally shown to have TPS activity, based

on in vitro activity measurements and yeast complementation assays (Blázquez et al., 1998; Harthill et al., 2006; Lunn, 2007; Ramon et al., 2009; Vandesteene et al., 2012). Although the subcellular location of the Arabidopsis TPS1 has not yet been experimentally determined, there is circumstantial evidence that it is restricted to the cytosol. The consensus of in silico prediction methods is that the TPS1 protein is cytosolic (http://suba.plantenergy.uwa.edu.au/; Tanz et al., 2012), and the TPS1 protein has not been detected so far in any proteomic analyses of Arabidopsis chloroplasts, mitochondria, or other organelles. Furthermore, when the N-terminal domain of the orthologous *Selaginella lepidophylla* TPS1 was fused to a GFP reporter, the fusion protein was not targeted to any recognizable organelle (Van Dijck et al., 2002). In our TPS29.2 and TPS31.3 lines, the *E. coli* TPS (otsA) protein has no recognizable transit or signal peptide and so is expected to be targeted to the cytosol. Therefore, Tre6P should also be synthesized only in the cytosol after induction of these plants with ethanol.

Nonaqueous fractionation of Arabidopsis rosettes indicated that 16% to 22% of the Tre6P is located in the chloroplasts, 71% to 72% in the cytosol, and 7% to 11% in the vacuoles (Table I). These estimates are based on the distributions of enzyme markers for the three compartments and computer fitting of the data to a three-compartment model using the BESTFIT algorithm (Klie et al., 2011). The algorithm assigned a similar percentage (66%–72%) of the Suc6P to the cytosol in both experiments (Table I). However, there is compelling evidence that Suc6P is restricted to the cytosol. The only enzymes known to metabolize Suc6P are SPS and Suc-phosphate phosphatase, both of which are strictly cytosolic (MacRae and Lunn, 2006, and refs. therein), and we are not aware of any reports of Suc6P transporters in plants that might allow the movement of Suc6P into other compartments. Thus, it seems reasonable to conclude that Suc6P is restricted to the cytosol and that the BESTFIT assignments based on marker enzymes overestimated the percentage of Suc6P in the chloroplasts and vacuole.

Tre6P showed an almost perfect correlation with Suc6P in the nonaqueous gradient fractions. It seems likely that the minor amounts of Tre6P assigned to the chloroplasts and vacuolar compartments by the BESTFIT algorithm reflect the technical limitations of the nonaqueous fractionation procedure and fitting of the data to a three-compartment model that does not take into account the different cell types within the leaf (i.e. palisade and spongy mesophyll, epidermis, stomatal guard cells, trichomes, and vascular tissue; Klie et al., 2011).

The subcellular in vivo concentrations of Tre6P in Arabidopsis mesophyll cells were estimated to be 3.81 to 6.71 μM in the cytosol, 0.18 to 0.46 μM in the chloroplasts, and 0.05 μM in the vacuole (Table I). For the reasons outlined above, the calculated concentrations of Tre6P in the chloroplasts and vacuole are likely to be overestimates and should be regarded as the upper limits of the Tre6P concentrations in these organelles. To our knowledge, these are the only experimentally based estimates of subcellular in vivo concentrations of Tre6P in plant cells to have been reported. We suggest that these estimates are a useful guide to the range of concentrations that should be used for in vitro experiments to investigate the targets of Tre6P signaling, and the physiological significance of any responses observed in vitro with much higher concentrations of Tre6P must be assessed with caution.

Regulation of Starch Synthesis by Tre6P

The rate of starch synthesis is determined by the rate of net CO_2 fixation and the partitioning of photoassimilates between starch and Suc. These pathways are controlled by a complex network of transcriptional, allosteric, and posttranslational mechanisms (for review, see MacRae and Lunn, 2006). According to the overflow hypothesis, starch is synthesized when the rate of photosynthesis exceeds the capacity of the leaf to export or store Suc (Cseke et al., 1994; Stitt et al., 2010). The original model proposed that rising levels of Suc in the leaf inhibit Suc synthesis, leading to an increase in the ratio of 3PGA to Pi in the chloroplast stroma, which stimulates starch synthesis via allosteric activation of AGPase (Cseke et al., 1994). Kolbe et al. (2005) extended the model by proposing that Tre6P mediates sugar-induced increases in the rate of starch synthesis via redox activation of AGPase. Lunn et al. (2006) observed parallel changes in Suc, Tre6P, and the redox status of AGPase in wild-type and mutant Arabidopsis rosettes, which appeared to be consistent with the proposed role of Tre6P. However, experimental evidence of a causal relationship between these parameters in vivo was lacking. We tested the hypothesis by investigating whether an induced rise in the level of Tre6P leads to reductive activation of AGPase and increased starch accumulation in the absence of any increase in Suc levels.

In three separate experiments, ethanol-induced overexpression of TPS led to a substantial (up to 11-fold) increase in the level of Tre6P (Fig. 1A; Supplemental Fig. S2, A and B). In two out of the three experiments, the induced plants accumulated a little more starch than the noninduced controls by the ED (Fig. 1B; Supplemental Fig. S2, C and D). The time course experiment suggested that there was a transient increase in the rate of starch accumulation from 4 to 6 h after induction (Fig. 1B), resulting in a higher ED starch content. The starch-Suc ratio showed a consistent trend to be higher in the induced TPS plants, even though Suc on its own was not significantly lower (Fig. 1, C and D; Supplemental Fig. S2, C, D, N, and O). The rates of net CO_2 assimilation in the induced TPS plants were indistinguishable from those in noninduced and AlcR control plants (Supplemental Fig. S5). Taken together, these results point toward a slight shift in photoassimilate partitioning in the induced TPS plants in favor of starch.

We found no consistent evidence of an increase in AGPase activation in the induced TPS plants. The redox status of AGPase after TPS induction was determined at the ED in three separate experiments, and no reproducible differences between induced and non-induced plants were observed (Fig. 1F; Supplemental Fig. S2, G and H). In one of these experiments, in which we examined the redox status of AGPase at time points throughout the day as well as at the ED, there appeared to be a transient ethanol effect in both the AlcR and TPS29.2 lines in the middle of the day (Fig. 1F). However, at every sampling time, the redox status of AGPase in the induced TPS plants overlapped with at least one, usually more, of the controls. It is also worth noting that during the period from 4 to 6 h after induction, when there was the clearest evidence of an increased rate of starch synthesis in the induced plants (Fig. 1B), the AGPase was, if anything, less reduced (i.e. less activated) in the induced plants (Fig. 1F). Furthermore, the induced and control plants contained very similar levels of ADPG not only at these time points but also at the later time points (Fig. 1E). From these results, we conclude that the induced increase in Tre6P led to a slight stimulation of starch synthesis, but this was not due to reductive activation of AGPase.

There are several potential explanations why AGPase activation was not increased in the induced TPS plants. One possibility is that the basal levels of Tre6P in the plants were already saturating the putative mechanism by which Tre6P affects the redox status of AGPase. The concentration of Tre6P in the cytosol was estimated to be 7 μM in wild-type plants grown in a 12-h photoperiod (Table I), presumably rising to 14 to 77 μM as a result of the 2- to 11-fold increase in Tre6P content observed in the induced TPS lines. However, in their isolated chloroplast experiments, Kolbe et al. (2005) reported that 100 μM Tre6P in the external medium was not quite saturating for the enzyme's response. Furthermore, Lunn et al. (2006) reported that AGPase was considerably more reduced in the *pgm* mutant, which had 3-fold higher levels of Tre6P and Suc, than in wild-type plants (Supplemental Fig. S4). Together, these observations suggest that the absence of a clear AGPase response in the induced TPS plants is not due to the mechanisms involved in redox modulation of AGPase being saturated by the levels of Tre6P already present in wild-type plants. Another possible explanation is that redox activation of AGPase requires the concerted action of two or more signaling pathways. Tre6P and Suc levels typically change in parallel (Lunn et al., 2006; Fig. 6). It is possible that a change in Tre6P levels is only effective when it is combined with other signaling events that are triggered when Suc rises. In any case, it appears that changes in the level of Tre6P on their own do not play a dominant role in regulating the redox status of AGPase in leaves.

It is also worthwhile noting that abolition of the redox sensitivity of AGPase by site-directed mutagenesis of APS1 had surprisingly little effect on the rate of starch synthesis in plants grown in a 12-h photoperiod (Hädrich et al., 2012). Thus, even if the induced increase in Tre6P had led to redox-related activation of AGPase, this might not have had much impact on the rate of starch synthesis.

At present, we can only speculate on possible mechanisms by which Tre6P brings about this small shift in photosynthate partitioning in favor of starch. The cytosolic Fru-1,6-bisphosphatase and SPS are considered to be the major sites for controlling Suc synthesis (MacRae and Lunn, 2006). The former is regulated by Fru-2,6-bisP, which is synthesized and degraded by a bifunctional kinase-phosphatase, which in turn is regulated allosterically and by protein phosphorylation. SPS is regulated by phosphorylation at multiple sites by SnRK1 and calcium-dependent protein kinases (Huber and Huber, 1996). SnRK1 from developing tissues is inhibited by micromolar concentrations of Tre6P (Zhang et al., 2009), but it seems unlikely that this sensitivity to Tre6P provides an explanation for a shift in photoassimilate partitioning in favor of starch synthesis. First, the SnRK1 activity in extracts from mature source leaves was found to be much less sensitive to inhibition by Tre6P (Zhang et al., 2009). Second, phosphorylation of the major SnRK1 target site (Ser-158 in spinach leaf SPS) deactivates the enzyme (Huber and Huber, 1996), so any inhibition of SnRK1 activity by Tre6P would be expected to activate, not inhibit, SPS and so favor Suc over starch synthesis.

In conclusion, our results indicate that Tre6P does have some influence over the rate of starch synthesis and photoassimilate partitioning. The change in

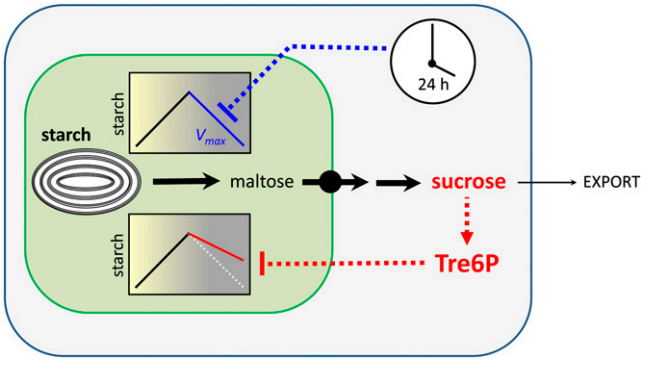

Figure 6. Integrated model of the control of starch breakdown by Tre6P and the circadian clock. The maximum permissible rate of starch degradation is set by the circadian clock to ensure that starch reserves are not exhausted before the expected dawn. If Suc export is restricted by low demand from sink organs, Suc accumulates in the leaves and Tre6P rises, leading to the inhibition of an early step in the pathway of starch degradation upstream of maltose production. As the core components of the clock operate in the nucleus, the pathway whereby it regulates starch breakdown presumably involves the transport of an unidentified signal into the chloroplast. Tre6P probably also inhibits starch breakdown via an intermediary that is formed in the cytosol and transmitted to the chloroplast.

partitioning, however, is relatively small compared with those that occur in response to other stimuli, such as short- or long-term changes in the photoperiod (Gibon et al., 2009; Hädrich et al., 2012). Furthermore, we found little evidence to support the hypothesis that Tre6P mediates Suc-induced activation of starch synthesis via reductive activation of AGPase. We suggest that the simplest interpretation of our results is that Suc-induced changes in the redox status of AGPase occur via a mechanism that does not involve Tre6P and that the correlation between Tre6P and the redox status of AGPase (Lunn et al., 2006) is driven by parallel but independent responses to Suc. Nevertheless, we cannot rule out the possibility that Tre6P can act to promote the activation of AGPase, but only in the presence of further signaling events that are initiated by an increase in Suc. Labeling experiments on the inducible TPS lines, using $^{13}CO_2$ or $^{14}CO_2$ to measure photosynthetic fluxes into Suc and starch (Szecowka et al., 2013), combined with measurements of Fru-2,6-bisP and the activation status of SPS would appear to be useful avenues for future research to understand how Tre6P influences photoassimilate partitioning.

Inhibition of Starch Degradation Mediated by Tre6P

Induced increases in the Tre6P content of Arabidopsis rosettes at night led to a strong inhibition of starch degradation, resulting in the plants retaining up to half of their starch reserves at the EN (Fig. 2). This contrasts markedly with the relatively weak effect on starch synthesis and points to Tre6P playing a major role in the regulation of starch breakdown.

Tre6P acts at an early step in starch breakdown. Maltose is the predominant product of starch breakdown in Arabidopsis leaves and is exported from the chloroplasts to the cytosol, where it provides substrates for Suc synthesis, respiration, and other processes (Niittylä et al., 2004; Weise et al., 2004). The *mex1* and *dpe2* mutants contain high levels of maltose, due to blocks in maltose export from the chloroplasts and catabolism in the cytosol, respectively (Chia et al., 2004; Lu and Sharkey, 2004; Niittylä et al., 2004). The *dpe1* mutant accumulates maltotriose and maltotetraose in the chloroplasts, as it is unable to metabolize these maltooligosaccharides (Critchley et al., 2001). While maltose rose rapidly in the dark as starch began to be degraded in wild-type or noninduced control plants (Figs. 3, D and H, and 5B), this increase was abolished or greatly attenuated in the induced plants with high Tre6P (Figs. 2G and 3, D and H), which contained 2- to 3-fold lower maltose levels than those in wild-type plants at the same time of the night. Induced TPS plants also had less maltotriose than the controls (Fig. 2H; Supplemental Figs. S8F and S9F). From these results, we conclude that Tre6P must be acting, directly or indirectly, to inhibit the pathway of starch degradation at some point upstream of maltose production.

There is considerable redundancy between the main starch debranching enzymes that are involved in starch degradation (isoamylase3 and limit dextrinase), and their functions can be at least partially replaced by the plastidial α-amylase (Streb et al., 2012). Therefore, unless Tre6P inhibits all three enzymes, it seems unlikely that the starch debranching process is the primary target of Tre6P. This leaves us with the earliest steps in starch degradation as the most likely targets for the inhibitory effect of high Tre6P: (1) the cycle of phosphorylation by GWD and PWD and dephosphorylation by SEX4 and LSF2, and (2) glucan chain exohydrolysis by β-amylase (especially BAM3).

Starch granules isolated from noninduced TPS29.2 plants had the typical discoid structure of Arabidopsis leaf starch, with a smooth surface. In contrast, the starch granules from induced plants had an irregular surface (Supplemental Fig. S12). This might indicate that binding of the starch-degrading enzymes is disrupted or blocked over large areas of the granule surface, preventing the more even pattern of degradation usually observed in Arabidopsis leaf starch granules.

Starch granules isolated from induced TPS29.2 plants generally had a higher phosphate content than those from noninduced plants and were found to be a poorer substrate for phosphorylation by recombinant GWD and PWD in vitro (Fig. 4). It should be noted that our measurements of phosphate content would include phosphate groups embedded within the granule as well as those on the surface of the granule, the latter being the most likely to influence further phosphorylation by GWD and PWD and hydrolysis of the glucan chains by β-amylase. In the noninduced control plants, both the C6-phosphate and total phosphate contents showed a tendency to decline through the night (Fig. 4). The surface area-to-volume ratio of the granules increases as the granules are degraded and become smaller, so the falling phosphate content indicates that the density of phosphorylated sites on the surface of the granules in the noninduced plants is likely to decrease through the night. In contrast, both the C6-phosphate and total phosphate content remained fairly constant in the starch granules from the induced TPS plants.

One explanation for both the inhibition of starch degradation and the observed differences in phosphate content could be the perturbation of the cycle of starch phosphorylation (by GWD and PWD) and dephosphorylation (by SEX4 and LSF2) by high Tre6P. An alternative explanation might be the inhibition of β-amylase by Tre6P. If the starch granules were not degraded due to inhibition of this enzyme, their surface area and volume, and by implication their phosphate content, would remain unchanged. It is also possible that a phosphorylation-dependent alteration of the structure of the granule surface could affect both the hydrolytic degradation of the starch and/or the (de)phosphorylation cycle.

We found no evidence of changes in the amounts of the GWD, PWD, or SEX4 proteins in the induced TPS

plants (Supplemental Figs. S10 and S11). In vitro assays indicated that GWD, PWD, SEX4, and BAM3 are insensitive to Tre6P (Supplemental Table S1; data not shown), even at concentrations (0.5–1.0 mM) that are 1,000 to 5,000 times higher than the estimated concentration of Tre6P in the chloroplasts in vivo (Table I). These enzymes also showed little sensitivity to trehalose.

Failure to detect changes in the in vitro activities of these enzymes in the presence of Tre6P must be interpreted with caution, as it is possible that factors needed for a response to Tre6P were absent from the in vitro assays. However, the simplest conclusion is that these enzymes are not directly sensitive to Tre6P. In this context, it is worth considering whether they would even encounter Tre6P in vivo. We estimated the in vivo concentration of Tre6P in the chloroplasts to be 0.18 to 0.46 μM (Table I), but, for the reasons discussed above, even these very low values might be an overestimate, and the possibility that there is no Tre6P in the chloroplasts cannot be excluded. Based on the subcellular compartmentation of Tre6P, it seems more likely that Tre6P triggers a response in the cytosol or at the surface of the chloroplasts, which subsequently leads to an inhibition of starch breakdown, rather than acting directly on the enzymes involved in starch degradation within the chloroplast.

In summary, we found several lines of evidence that Tre6P acts to inhibit one or more of the early steps in the starch degradation pathway within the chloroplast, probably indirectly via a signaling pathway that is initiated in the cytosol: (1) the majority, perhaps even all, of the Tre6P in Arabidopsis leaves is located in the cytosol; (2) induced TPS plants have low maltose, pointing to inhibition of an early reaction in starch breakdown; (3) there is no accumulation of maltotriose, ruling out inhibition of the chloroplastic DPE1; and (4) there are changes in the visual appearance and the phosphorylation status of the starch granules. Whatever the mechanism, we suggest that inhibition of starch degradation by Tre6P is likely to be an important factor underlying the high-starch phenotype observed in Arabidopsis plants with constitutive overexpression of TPS (Schluepmann et al., 2003; Kolbe et al., 2005) and probably more important than stimulation of starch synthesis by Tre6P.

The Inhibition of Starch Degradation by Tre6P Results in a Decrease in Suc Levels during the Night

The inhibition of starch degradation in induced TPS plants with increased Tre6P was accompanied by a decrease in Suc levels during the night (Figs. 2C and 3, C and G). These plants also had less Suc6P (Supplemental Figs. S8E and S9E), which is consistent with the lower Suc being due to decreased synthesis rather than increased use of Suc. The decrease in Suc was most pronounced between 4 and 6 h into the night. The difference between induced and noninduced plants became smaller toward the EN as Suc levels gradually declined in the control plants, coinciding with the gradual depletion of starch. In our time-course experiments, the first time point analyzed during the night was at 2 h after dusk. At this time, Tre6P was significantly higher in the induced plants, while Suc and maltose levels were lower than in noninduced plants (Fig. 3). The starchless *pgm* mutant does not accumulate maltose at night (Niittylä et al., 2004), and β-amylase-deficient mutants that degrade their starch more slowly than wild-type plants have lower maltose levels than the wild type during the first half of the night (Fulton et al., 2008). These observations indicate that the rise in maltose levels in wild-type plants after dusk is dependent on starch breakdown. Thus, the low maltose in the induced TPS plants at 2 h after dusk provides indirect evidence that starch breakdown is already inhibited in these plants, even if this is not obvious from the starch measurements themselves. It should be noted that rates of starch degradation inferred from the differences in starch content at successive time points lack precision, especially during the early hours of the night, when starch content is high and small differences in starch content are more difficult to observe because of the technical limitations of the starch assay. For this reason, we suggest that maltose content is a more reliable guide to the rate of starch breakdown during the early hours of the night, and the low maltose levels in the induced TPS plants at 2 h after dusk indicate that starch breakdown is already inhibited by Tre6P at this time. Inhibition of starch degradation will restrict the supply of substrates for Suc synthesis, offering a simple explanation for the lower Suc content of the induced TPS plants.

An alternative explanation for the low level of Suc in the induced lines might be that high Tre6P has stimulated Suc consumption. Tre6P has been proposed to stimulate growth by inhibiting the SnRK1 protein kinase in developing tissues (Zhang et al., 2009; Debast et al., 2011). Higher growth rates at night would be expected to increase the respiration of Suc to provide the energy and carbon skeletons needed for growth, potentially explaining the lower Suc levels in the induced TPS plants. However, we found that induced TPS plants did not have significantly higher dark respiration rates (Supplemental Fig. S6). In fact, if anything, respiration rates showed a tendency to be lower after induction of the TPS plants. Polysome loading, a proxy for protein synthesis, also did not increase after induction of the TPS plants (Supplemental Fig. S7) and even showed a tendency to be lower in the induced plants at 2 and 4 h after dusk. This coincides with the time when the differences in maltose and Suc content became apparent (Fig. 3). As respiration and protein synthesis are major requirements for growth, these results argue against increased Suc consumption, resulting from a stimulation of growth by Tre6P, being the primary cause of the low Suc levels in the induced TPS plants at night.

Control of Starch Mobilization by the Circadian Clock Also Involves the Inhibition of an Early Step in the Pathway of Starch Degradation

There is compelling evidence that the circadian clock plays a major role in the control of nighttime starch degradation (Lu et al., 2005; Graf et al., 2010; Graf and Smith, 2011). If wild-type Arabidopsis plants growing under 12-h-light/12-h-dark conditions are darkened several hours before the usual dusk, they not only start the night with a lower amount of starch but also face a longer night than usual. Despite this, they still manage to degrade their starch in a linear manner at a rate that avoids them running out of starch before the EN (Graf et al., 2010). This adjustment implies that the plant is able to measure the amount of starch present in the leaves and predict the length of the night, the latter being a potential readout of the circadian clock (Graf and Smith, 2011; Stitt and Zeeman, 2012). The mechanisms by which the plant measures its starch content and sets the rate of degradation are unknown, although modeling has provided a conceptual framework for understanding how the necessary calculation (i.e. starch divided by time) might be achieved (Scialdone et al., 2013).

The regulation of starch breakdown by the clock is important for the optimization of plant growth. Wild-type plants grown in abnormally short (20 h) or long (28 h) light/dark cycles mistime their starch turnover during the night (Graf et al., 2010) and grow more slowly than control plants in a 24-h light/dark cycle (Dodd et al., 2005). In contrast, the short-period-clock mutant *cca1/lhy* exhausts its starch reserves before the EN, grows more slowly than wild-type plants when grown under 12-h-light/12-h-dark conditions (Graf et al., 2010), and grows better in a 10-h-light/10-h-dark cycle, in which the plants are reilluminated before their starch reserves run out (Dodd et al., 2005). Yazdanbakhsh et al. (2011) showed that the premature exhaustion of starch in the *cca1/lhy* mutant under 12-h-light/12-h-dark conditions is accompanied by an inhibition of root growth at the EN and that this inhibition can be reversed by exogenous supply of Suc. Thus, under optimal growth conditions, it appears to be advantageous for the plant to time its remobilization of transitory starch so that it avoids premature depletion of these reserves before the EN.

It is not yet known how the clock regulates starch turnover, whether it acts in a direct or indirect manner, and whether Tre6P is directly involved or not. One hypothetical example of an indirect mechanism would be for the clock to restrict growth, resulting in the accumulation of sugars, an increase of Tre6P, and inhibition of starch breakdown. A clock-driven increase in Tre6P leading to the inhibition of starch degradation, independently of changes in Suc, is also conceivable. To distinguish between these possibilities, we repeated the early-dusk experiment of Graf et al. (2010). The lower rate of starch degradation after an early dusk was accompanied by: (1) lower levels of Tre6P; (2) lower levels of intermediates in the starch breakdown pathway (maltose and maltotriose); and (3) lower levels of the products of starch breakdown and related metabolites (Suc, Glc6P, and Suc6P; Fig. 5; Supplemental Fig. S14). These results provide evidence that the clock regulates starch breakdown by acting at an early step in the pathway, upstream of maltose. Most importantly, the lower Tre6P levels after the early dusk show that Tre6P is not an intermediate in the clock-dependent signaling pathway that sets an appropriate rate of starch degradation for the expected length of the night. If anything, the lower level of Tre6P would be expected to allow a faster rate of starch degradation due to the lifting of the inhibitory effect of this metabolite.

The Clock and Tre6P Interact to Regulate Starch Breakdown

We propose that the clock and Tre6P interact to determine the rate of starch degradation (Fig. 6). The clock paces the mobilization of starch to ensure that starch reserves are not exhausted before the EN. However, it is important to note that under growth conditions that allow large amounts of carbon to be fixed during the day (e.g. high light and long days) or that restrict growth at night, the plant might not use up all of its starch reserves by dawn (Hädrich et al., 2012; Stitt and Zeeman, 2012). The implication is that the clock sets a maximum permissible rate of starch degradation but does not drive a faster rate of starch degradation than is necessary to supply the Suc needed for growth and maintenance. We propose that Tre6P plays a significant role in matching the rate of starch breakdown with Suc use. If the environmental conditions during the night are unfavorable for growth (e.g. low temperature, limiting nutrients), lower demand for Suc by growing sink organs may limit Suc export from the source leaves. The resulting accumulation of Suc will trigger a rise in the level of Tre6P, as this signal metabolite closely tracks any fluctuations in the level of Suc (Fig. 5; Lunn et al., 2006), resulting in an inhibition of starch degradation. In this way, the plant would avoid remobilizing its starch reserves unnecessarily when the carbon is not needed to support growth. Conversely, if conditions become more favorable for growth and demand for Suc exceeds the supply from starch breakdown, both Suc and Tre6P levels would fall, lifting the inhibition of starch degradation. However, the rate of starch breakdown will not be allowed to rise above the maximum limit set by the clock. In summary, our model envisages the rate of starch breakdown to be jointly regulated by the circadian clock and Tre6P, with the clock-dependent regulation preventing premature exhaustion of starch before dawn, while Tre6P links the rate of degradation to the demand for Suc.

MATERIALS AND METHODS

Plant Material

The *Escherichia coli otsA* gene (GenBank accession no. X69160) encoding TPS (EC 2.4.1.15) was cloned into the *Spe*I site of the pSRN binary vector (Caddick et al., 1998), downstream of the *AlcA* promoter. The resulting construct was introduced into Arabidopsis (*Arabidopsis thaliana*) accession Col-0 via *Agrobacterium tumefaciens* transformation using the floral dip method (Clough and Bent, 1998). A control line (AlcR) expressing only the AlcR transcription factor was generated by transforming Arabidopsis Col-0 with the empty pSRN plasmid. Primary transformants were selected on one-half-strength Murashige and Skoog medium (Murashige and Skoog, 1962) containing 50 mg L^{-1} kanamycin. Kanamycin-resistant pSRN/*otsA* plants were further screened for ethanol-inducible expression of the otsA protein by immunoblotting. T2 progeny from the primary transformants were screened by kanamycin selection, and lines showing segregation patterns consistent with the presence of a single transgenic locus (3:1 kanamycin resistant:kanamycin sensitive) were rescreened in the T3 generation to identify homozygous T2 lines.

Plant Growth Conditions and Ethanol Induction

Seeds from Arabidopsis were sown on soil mixed with vermiculite (1:1) in 10-cm pots and placed for 1 week in a phytotron under long-day conditions, 16 h (20°C) of light/8 h (4°C) of dark, with an irradiance of 160 μE m^{-2} s^{-1}. In the second week, pots were transferred to a short-day phytotron, 8 h (20°C) of light/16 h (16°C) of dark, at the same irradiance. At 2 weeks after sowing, seedlings were transplanted into 10-cm pots (five plants per pot) and transferred to equinoctial conditions (12 h of light/12 h of dark) at constant 20°C, with an irradiance of 130 μE m^{-2} s^{-1}, until harvest.

Four-week-old plants were sprayed to runoff with water (mock induction control) or 2% (v/v) ethanol and harvested at various times from 2 to 18 h after spraying, as indicated for each individual experiment. Whole rosettes were excised under the ambient growth conditions and immediately quenched in liquid nitrogen. Plants from one or two pots (i.e. five or 10 plants) were pooled to form one sample, ground to a fine powder at −70°C using a robotized ball mill (Stitt et al., 2007), and stored at −80°C until use.

Extraction and Measurement of Metabolites

Soluble sugars (Glc, Fru, and Suc) were extracted with ethanol and enzymatically assayed according to Stitt et al. (1989). Starch was determined enzymatically in the insoluble material after ethanolic extraction of soluble sugars (Hendriks et al., 2003). Tre6P and phosphorylated intermediates were extracted in chloroform-methanol and measured by high-performance anion-exchange chromatography coupled to tandem mass spectrometry (LC-MS/MS) as described by Lunn et al. (2006) using a Finnigan TSQ Quantum (ThermoFinnigan) or a QTrap 5500 MS-Q3 (AB Sciex) triple quadrupole mass spectrometer. Tre6P was quantified using enzymatically calibrated standards and a [^{2}H]Tre6P internal standard to correct for ion suppression and matrix effects (Lunn et al., 2006). Trehalose was quantified fluorimetrically in the same chloroform-methanol extract as described by Carillo et al. (2013).

Maltose and maltotriose were measured using a modification of the method described by Fulton et al. (2008). The extraction was performed with 1.5 N perchloric acid, and the extract was neutralized with 2 N KOH/0.4 M MES/0.4 M KCl. The neutral fraction was separated and analyzed by high-pressure anion-exchange chromatography on a CarboPac PA-100 4- × 250-mm column (ThermoFisher) with pulsed amperometric detection as described by Fulton et al. (2008). Maltose and maltotriose were identified and quantified by comparison with original standards (Carbosynth) using Chromeleon software (version 6.8; ThermoFisher).

Nonaqueous Fractionation

Frozen tissue powder was lyophilized and fractionated by centrifugation on anhydrous hexane-tetrachloroethylene gradients as described by Gerhardt and Heldt (1984), with the modifications for Arabidopsis leaf material described by Krueger et al. (2009). The following markers were used in the experiments reported in Table I: for chloroplasts, AGPase and Rubisco in experiment 1 and transketolase and phosphoribulokinase in experiment 2; for cytosol, UDP-Glc pyrophosphorylase and phospho*enol*pyruvate carboxylase in both experiments; and for vacuole, acid invertase in both experiments, nitrate in experiment 1, and α-glucosidase in experiment 2. The subcellular distribution of Tre6P between chloroplasts, cytosol, and vacuoles was calculated using the BESTFIT program (Klie et al., 2011).

Native PAGE

Soluble proteins were extracted from 200 mg of powdered frozen leaf material with 1 mL of extraction buffer containing 50 mM HEPES-NaOH buffer (pH 7.5), 1 mM EDTA, 5 mM dithioerythritol, 0.5 mM phenylmethanesulfonyl fluoride, and 10% (v/v) glycerol. Following centrifugation (12,000*g* for 10 min at 4°C), aliquots of the supernatant were assayed for total protein content (Bradford, 1976). For analysis of cytosolic disproportionating enzyme (DPE2) and cytosolic/chloroplastic phosphorylase (PHS2 and PHS1) activities, aliquots containing 20 μg of protein were separated by native PAGE under nondenaturing conditions, as described by Steup (1990). Electrophoresis was performed at 4°C at constant 250 V, and the separating gels were stained according Fettke et al. (2005).

Immunoblotting

A His_6-tagged otsA protein was overexpressed in *E. coli* and purified by metal ion affinity chromatography and gel filtration (otsA) as described by Lunn et al. (2006). Antisera were raised by immunization of rabbits with the purified otsA protein. Antibodies were purified by affinity chromatography on an otsA-Sepharose column, generated by coupling the His_6-otsA protein to a 1-mL HiTrap *N*-hydroxysuccinimide-activated HP Sepharose prepacked column (GE Healthcare Biosciences). SDS-PAGE and immunoblotting with nitroblue tetrazolium/5-bromo-4-chloro-3-indolyl phosphate colorimetric detection was carried out as described by Lunn et al. (1999) using the antiotsA antibody at a 1:20,000 dilution. Quantification of GWD, PWD, and SEX4 (Niittylä et al., 2006) proteins by immunoblotting was performed as described by Fettke et al. (2004).

The redox status of AGPase was determined by immunoblotting of leaf proteins after SDS-PAGE under nonreducing conditions as described by Hendriks et al. (2003). Leaf extracts from the wild-type Col-0 and the starch-deficient *pgm* mutant were included as controls on each gel to allow correction for blot-to-blot variation. Quantitative detection of the Arabidopsis APS1 protein was performed using the Odyssey infrared imaging system (LiCor) as described by Hädrich et al. (2012). The percentage of total APS1 protein present as the 50-kD monomer was determined for each sample after subtraction of the background. For each individual immunoblot, the percentage monomer values from the wild-type Col-0 and *pgm* samples were compared with the averages for those samples across all the immunoblots and used to calculate a linear scaling factor for normalization of the other samples.

Starch Granule Isolation and Scanning Electron Microscopy

Powdered frozen leaves (15–20 g) were extracted in 50 mL of extraction buffer (20 mM HEPES-KOH, 0.4 mM EDTA, and 0.5% [v/v] Triton X-100, pH 7.5) using a 250-mL goblet blender. The homogenate was filtered sequentially through nylon nets with mesh sizes of 100, 20, and 15 μm, and the final filtrate was centrifuged at 1,000*g* (4°C) for 5 min. The supernatant was discarded, and the pellet was washed twice by resuspension in 15 mL of extraction buffer and centrifugation. The resulting pellet was suspended in 500 μL of water, layered on top of a 15-mL cushion of 95% (v/v) Percoll (GE Healthcare Bio-Sciences) in water, and centrifuged at 2,000*g* (4°C) for 15 min. After centrifugation, the Percoll cushion was discarded, and the pelleted starch granules were washed three times by resuspension in 30 mL of water and centrifuged at 1,000*g* (4°C) for 5 min. The final pellet was then frozen in liquid nitrogen and lyophilized. The surface structure of the starch granules was examined with a Quanta 200 scanning electron microscope (FEI; http://www.fei.com) after sputter coating of the granules with gold under a low vacuum.

Determination of Starch Phosphate Content

About 6 mg of isolated starch granules was hydrolyzed by incubation with 300 μL of 0.7 N HCl for 4 h at 95°C. After neutralization with 1.8 N NaOH containing 0.2 mM Tris (base), Glc and Glc6P were determined enzymatically according to Stitt et al. (1989). To determine total phosphate content, aliquots

of 200 μL of the hydrolyzed starch were incubated in a reaction mixture (final volume, 300 μL) containing 100 mM Tris-HCl (pH 9.5), 100 mM NaCl, 5 mM $MgCl_2$, and 20 units of alkaline phosphatase for 1 h at 37°C, and Pi was measured colorimetrically using malachite green reagent (Harder et al., 1994; Worby et al., 2006).

Incorporation of Phosphate into Starch by Recombinant GWD and PWD

Isolated starch granules (about 30 mg) were suspended in 1 mL of water. Aliquots (188 μL) of the suspension were incubated in a reaction mixture (final volume, 250 μL) containing 50 mM HEPES-KOH, pH 7.5, 6 mM $MgCl_2$, 2 mM EDTA, 2 mM DTT, 25 μM ATP, 1 μCi of [β-^{33}P]ATP, 20 μg of bovine serum albumin, 0.1 μg of recombinant GWD from potato (*Solanum tuberosum*; StGWD), and 0.1 μg of recombinant PWD from Arabidopsis (AtPWD). The reaction mixture was incubated at 30°C with continuous agitation for 25 min. Every 5 min, 50-μL samples were removed and mixed with 50 μL of 10% (w/v) SDS to stop the reaction. The starch granules were pelleted by centrifugation at 10,000*g* at room temperature for 5 min. The supernatant was discarded, and the pellet was washed five times by resuspension in 1 mL of 5 mM HEPES-KOH, pH 7.4, containing 2 mM ATP and centrifugation as described above. The washed granules were resuspended in 100 μL of water before the addition of 3 mL of scintillation cocktail and the determination of radioactivity by liquid scintillation counting, using an external standard to correct for quenching (Hejazi et al., 2008).

Enzyme Assays

GWD

GWD activity was assayed by measuring the incorporation of ^{33}P from [β-^{33}P]ATP into the B-type allomorph of crystallized maltodextrin (MD_{cryst}). The reaction (final volume, 100 μL) contained 50 mM HEPES-KOH (pH 7.5), 6 mM $MgCl_2$, 2 mM EDTA, 2 mM dithioerythritol, 25 μM unlabeled ATP, 1 μCi of [β-^{33}P]ATP, 20 μg of bovine serum albumin, with 4 mg of MD_{cryst} as substrate, and 0.5 μg of recombinant StGWD. The reaction mixture was incubated at 30°C with continuous agitation. Aliquots (50 μL) were taken at 2.5, 5, 10, and 20 min and heated at 95°C for 3 min to stop the reaction, and the incorporation of ^{33}P was determined as described by Hejazi et al. (2008).

PWD

PWD activity was assayed by measuring the incorporation of ^{33}P from [β-^{33}P]ATP into B-type MD_{cryst} that had been prephosphorylated by incubation with unlabeled ATP and StGWD (Hejazi et al., 2008). The basic PWD assay reaction mixture was identical to that described above for GWD above, except that 4 mg of phosphorylated MD_{cryst} was used as the substrate and the StGWD was replaced by 0.5 μg of recombinant AtPWD.

SEX4 Phosphoglucan Phosphatase

SEX4 activity was assayed by measuring the release of ^{33}P from A-type MD_{cryst} that had been prephosphorylated by incubation with [β-^{33}P]ATP and StGWD as described above. The reaction contained recombinant SEX4 enzyme from Arabidopsis (AtSEX4) and was carried out as described by Hejazi et al. (2010).

Sequence data from this article can be found in the GenBank/EMBL data libraries under accession number X69160 (*otsA*).

Supplemental Data

The following materials are available in the online version of this article.

Supplemental Figure S1. Inducible expression of *E. coli* otsA (TPS) in Arabidopsis.

Supplemental Figure S2. Effect of TPS overexpression on the metabolite content of Arabidopsis rosettes during the day.

Supplemental Figure S3. Immunoblotting of the APS1 protein in Arabidopsis leaf extracts to determine the redox status of AGPase.

Supplemental Figure S4. Effect of TPS overexpression on the metabolite content of Arabidopsis rosettes during the day.

Supplemental Figure S5. Effect of induced changes in Tre6P on photosynthetic CO_2 assimilation in Arabidopsis.

Supplemental Figure S6. Effect of induced changes in Tre6P on dark respiration in Arabidopsis rosettes.

Supplemental Figure S7. Effect of Tre6P on polysome loading in Arabidopsis rosettes at night.

Supplemental Figure S8. Effect of inducing Tre6P synthesis at the ED on metabolite levels during the following night.

Supplemental Figure S9. Effect of inducing Tre6P synthesis in the middle of the day on metabolite levels during the following night.

Supplemental Figure S10. Effect of induced changes in Tre6P on enzymes involved in starch degradation in Arabidopsis rosettes.

Supplemental Figure S11. Effect of induced changes in Tre6P on the SEX4 phosphoglucan phosphatase in Arabidopsis rosettes.

Supplemental Figure S12. Scanning electron micrographs of starch granules isolated from induced and noninduced TPS29.2 plants.

Supplemental Figure S13. Subcellular compartmentation of Tre6P in Arabidopsis rosettes.

Supplemental Figure S14. Effect of an early dusk on metabolite levels in Arabidopsis leaves.

Supplemental Table S1. Effect of Tre6P and trehalose on the in vitro activity of enzymes involved in starch degradation.

ACKNOWLEDGMENTS

We thank Dr. Karin Köhl, Christin Abel, and the Max Planck Institute of Molecular Plant Physiology greenhouse staff for advice and help with plant cultivation, Prof. Alison Smith (John Innes Centre) and Dr. Hendrik Poorter (Forschungszentrum Jülich) for helpful discussions on starch metabolism and leaf anatomy, and Dr. Zoran Nikoloski (Max Planck Institute of Molecular Plant Physiology) for advice on data analysis.

Received August 14, 2013; accepted September 16, 2013; published September 16, 2013.

LITERATURE CITED

Andriotis VME, Pike MJ, Schwarz SL, Rawsthorne S, Wang TL, Smith AM (2012) Altered starch turnover in the maternal plant has major effects on Arabidopsis fruit growth and seed composition. Plant Physiol **160:** 1175–1186

Arrivault S, Guenther M, Ivakov A, Feil R, Vosloh D, van Dongen JT, Sulpice R, Stitt M (2009) Use of reverse-phase liquid chromatography, linked to tandem mass spectrometry, to profile the Calvin cycle and other metabolic intermediates in Arabidopsis rosettes at different carbon dioxide concentrations. Plant J **59:** 826–839

Ballicora MA, Frueauf JB, Fu Y, Schürmann P, Preiss J (2000) Activation of the potato tuber ADP-glucose pyrophosphorylase by thioredoxin. J Biol Chem **275:** 1315–1320

Baunsgaard L, Lütken H, Mikkelsen R, Glaring MA, Pham TT, Blennow A (2005) A novel isoform of glucan, water dikinase phosphorylates prephosphorylated α-glucans and is involved in starch degradation in Arabidopsis. Plant J **41:** 595–605

Blázquez MA, Santos E, Flores CL, Martínez-Zapater JM, Salinas J, Gancedo C (1998) Isolation and molecular characterization of the Arabidopsis *TPS1* gene, encoding trehalose-6-phosphate synthase. Plant J **13:** 685–689

Blennow A, Engelsen SB (2010) Helix-breaking news: fighting crystalline starch energy deposits in the cell. Trends Plant Sci **15:** 236–240

Blennow A, Nielsen TH, Baunsgaard L, Mikkelsen R, Engelsen SB (2002) Starch phosphorylation: a new front line in starch research. Trends Plant Sci **7:** 445–450

Bradford MM (1976) A rapid and sensitive method for the quantitation of microgram quantities of protein utilizing the principle of protein-dye binding. Anal Biochem **72:** 248–254

Caddick MX, Greenland AJ, Jepson I, Krause KP, Qu N, Riddell KV, Salter MG, Schuch W, Sonnewald U, Tomsett AB (1998) An ethanol inducible gene switch for plants used to manipulate carbon metabolism. Nat Biotechnol **16:** 177–180

Carillo P, Feil R, Gibon Y, Satoh-Nagasawa N, Jackson D, Bläsing OE, Stitt M, Lunn JE (2013) A fluorometric assay for trehalose in the picomole range. Plant Methods **9:** 21–35

Chatterton NJ, Silvius JE (1980) Photosynthate partitioning into leaf starch as affected by daily photosynthetic period duration in six species. Physiol Plant **49:** 141–144

Cheng SH, Moore B, Seemann JR (1998) Effects of short- and long-term elevated CO_2 on the expression of ribulose-1,5-bisphosphate carboxylase/oxygenase genes and carbohydrate accumulation in leaves of *Arabidopsis thaliana* (L.) Heynh. Plant Physiol **116:** 715–723

Chia T, Thorneycroft D, Chapple A, Messerli G, Chen J, Zeeman SC, Smith SM, Smith AM (2004) A cytosolic glucosyltransferase is required for conversion of starch to sucrose in Arabidopsis leaves at night. Plant J **37:** 853–863

Cho MH, Lim H, Shin DH, Jeon JS, Bhoo SH, Park YI, Hahn TR (2011) Role of the plastidic glucose translocator in the export of starch degradation products from the chloroplasts in *Arabidopsis thaliana*. New Phytol **190:** 101–112

Clough SJ, Bent AF (1998) Floral dip: a simplified method for *Agrobacterium*-mediated transformation of *Arabidopsis thaliana*. Plant J **16:** 735–743

Comparot-Moss S, Kötting O, Stettler M, Edner C, Graf A, Weise SE, Streb S, Lue W-L, MacLean D, Mahlow S, et al (2010) A putative phosphatase, LSF1, is required for normal starch turnover in Arabidopsis leaves. Plant Physiol **152:** 685–697

Critchley JH, Zeeman SC, Takaha T, Smith AM, Smith SM (2001) A critical role for disproportionating enzyme in starch breakdown is revealed by a knock-out mutation in Arabidopsis. Plant J **26:** 89–100

Cseke C, Balogh A, Wong JH, Buchanan BB, Stitt M, Herzog B, Heldt HW (1994) Fructose 2,6-bisphosphate: a regulator of carbon processing in leaves. Trends Biochem Sci **9:** 533–535

Debast S, Nunes-Nesi A, Hajirezaei MR, Hofmann J, Sonnewald U, Fernie AR, Börnke F (2011) Altering trehalose-6-phosphate content in transgenic potato tubers affects tuber growth and alters responsiveness to hormones during sprouting. Plant Physiol **156:** 1754–1771

de Dios Barajas-López J, Tezycka J, Travaglia CN, Serrato AJ, Chueca A, Thormählen I, Geigenberger P, Sahrawy M (2012) Expression of the chloroplast thioredoxins f and m is linked to short-term changes in the sugar and thiol status in leaves of *Pisum sativum*. J Exp Bot **63:** 4887–4900

Dodd AN, Salathia N, Hall A, Kévei E, Tóth R, Nagy F, Hibberd JM, Millar AJ, Webb AA (2005) Plant circadian clocks increase photosynthesis, growth, survival, and competitive advantage. Science **309:** 630–633

Edner C, Li J, Albrecht T, Mahlow S, Hejazi M, Hussain H, Kaplan F, Guy C, Smith SM, Steup M, et al (2007) Glucan, water dikinase activity stimulates breakdown of starch granules by plastidial β-amylases. Plant Physiol **145:** 17–28

Fettke J, Chia T, Eckermann N, Smith A, Steup M (2006) A transglucosidase necessary for starch degradation and maltose metabolism in leaves at night acts on cytosolic heteroglycans (SHG). Plant J **46:** 668–684

Fettke J, Eckermann N, Poeste S, Pauly M, Steup M (2004) The glycan substrate of the cytosolic (Pho 2) phosphorylase isozyme from *Pisum sativum* L.: identification, linkage analysis and subcellular localization. Plant J **39:** 933–946

Fettke J, Hejazi M, Smirnova J, Höchel E, Stage M, Steup M (2009) Eukaryotic starch degradation: integration of plastidial and cytosolic pathways. J Exp Bot **60:** 2907–2922

Fettke J, Poeste S, Eckermann N, Tiessen A, Pauly M, Geigenberger P, Steup M (2005) Analysis of cytosolic heteroglycans from leaves of transgenic potato (*Solanum tuberosum* L.) plants that under- or overexpress the Pho 2 phosphorylase isozyme. Plant Cell Physiol **46:** 1987–2004

Fu Y, Ballicora MA, Leykam JF, Preiss J (1998) Mechanism of reductive activation of potato tuber ADP-glucose pyrophosphorylase. J Biol Chem **273:** 25045–25052

Fulton DC, Stettler M, Mettler T, Vaughan CK, Li J, Francisco P, Gil M, Reinhold H, Eicke S, Messerli G, et al (2008) β-AMYLASE4, a noncatalytic protein required for starch breakdown, acts upstream of three active β-amylases in *Arabidopsis* chloroplasts. Plant Cell **20:** 1040–1058

Gerhardt R, Heldt HW (1984) Measurement of subcellular metabolite levels in leaves by fractionation of freeze-stopped material in nonaqueous media. Plant Physiol **75:** 542–547

Gibon Y, Bläsing OE, Palacios-Rojas N, Pankovic D, Hendriks JHM, Fisahn J, Höhne M, Günther M, Stitt M (2004) Adjustment of diurnal starch turnover to short days: depletion of sugar during the night leads to a temporary inhibition of carbohydrate utilization, accumulation of sugars and post-translational activation of ADP-glucose pyrophosphorylase in the following light period. Plant J **39:** 847–862

Gibon Y, Pyl ET, Sulpice R, Lunn JE, Höhne M, Günther M, Stitt M (2009) Adjustment of growth, starch turnover, protein content and central metabolism to a decrease of the carbon supply when Arabidopsis is grown in very short photoperiods. Plant Cell Environ **32:** 859–874

Glaring MA, Skryhan K, Kötting O, Zeeman SC, Blennow A (2012) Comprehensive survey of redox sensitive starch metabolising enzymes in *Arabidopsis thaliana*. Plant Physiol Biochem **58:** 89–97

Graf A, Schlereth A, Stitt M, Smith AM (2010) Circadian control of carbohydrate availability for growth in Arabidopsis plants at night. Proc Natl Acad Sci USA **107:** 9458–9463

Graf A, Smith AM (2011) Starch and the clock: the dark side of plant productivity. Trends Plant Sci **16:** 169–175

Hädrich N, Hendriks JHM, Kötting O, Arrivault S, Feil R, Zeeman SC, Gibon Y, Schulze WX, Stitt M, Lunn JE (2012) Mutagenesis of cysteine 81 prevents dimerization of the APS1 subunit of ADP-glucose pyrophosphorylase and alters diurnal starch turnover in Arabidopsis thaliana leaves. Plant J **70:** 231–242

Haebel S, Hejazi M, Frohberg C, Heydenreich M, Ritte G (2008) Mass spectrometric quantification of the relative amounts of C6 and C3 position phosphorylated glucosyl residues in starch. Anal Biochem **379:** 73–79

Harder KW, Owen P, Wong LKH, Aebersold R, Clark-Lewis I, Jirik FR (1994) Characterization and kinetic analysis of the intracellular domain of human protein tyrosine phosphatase β (HPTP β) using synthetic phosphopeptides. Biochem J **298:** 395–401

Harthill JE, Meek SEM, Morrice N, Peggie MW, Borch J, Wong BHC, Mackintosh C (2006) Phosphorylation and 14-3-3 binding of Arabidopsis trehalose-phosphate synthase 5 in response to 2-deoxyglucose. Plant J **47:** 211–223

Hejazi M, Fettke J, Haebel S, Edner C, Paris O, Frohberg C, Steup M, Ritte G (2008) Glucan, water dikinase phosphorylates crystalline maltodextrins and thereby initiates solubilization. Plant J **55:** 323–334

Hejazi M, Fettke J, Kötting O, Zeeman SC, Steup M (2010) The laforin-like dual-specificity phosphatase SEX4 from Arabidopsis hydrolyzes both C6- and C3-phosphate esters introduced by starch-related dikinases and thereby affects phase transition of α-glucans. Plant Physiol **152:** 711–722

Hendriks JHM, Kolbe A, Gibon Y, Stitt M, Geigenberger P (2003) ADP-glucose pyrophosphorylase is activated by posttranslational redox-modification in response to light and to sugars in leaves of Arabidopsis and other plant species. Plant Physiol **133:** 838–849

Huber SC, Huber JL (1996) Role and regulation of sucrose-phosphate synthase in higher plants. Annu Rev Plant Physiol Plant Mol Biol **47:** 431–444

Klie S, Krueger S, Krall L, Giavalisco P, Flügge UI, Willmitzer L, Steinhauser D (2011) Analysis of the compartmentalized metabolome: a validation of the non-aqueous fractionation technique. Front Plant Sci **2:** 55

Kolbe A, Tiessen A, Schluepmann H, Paul M, Ulrich S, Geigenberger P (2005) Trehalose 6-phosphate regulates starch synthesis via posttranslational redox activation of ADP-glucose pyrophosphorylase. Proc Natl Acad Sci USA **102:** 11118–11123

Kötting O, Kossmann J, Zeeman SC, Lloyd JR (2010) Regulation of starch metabolism: the age of enlightenment? Curr Opin Plant Biol **13:** 321–329

Kötting O, Pusch K, Tiessen A, Geigenberger P, Steup M, Ritte G (2005) Identification of a novel enzyme required for starch metabolism in Arabidopsis leaves: the phosphoglucan, water dikinase. Plant Physiol **137:** 242–252

Kötting O, Santelia D, Edner C, Eicke S, Marthaler T, Gentry MS, Comparot-Moss S, Chen J, Smith AM, Steup M, et al (2009) STARCH-EXCESS4 is a laforin-like phosphoglucan phosphatase required for starch degradation in *Arabidopsis thaliana*. Plant Cell **21:** 334–346

Krueger S, Niehl A, Lopez Martin MC, Steinhauser D, Donath A, Hildebrandt T, Romero LC, Hoefgen R, Gotor C, Hesse H (2009) Analysis of cytosolic and plastidic serine acetyltransferase mutants and

subcellular metabolite distributions suggests interplay of the cellular compartments for cysteine biosynthesis in Arabidopsis. Plant Cell Environ **32:** 349–367

Lu Y, Gehan JP, Sharkey TD (2005) Daylength and circadian effects on starch degradation and maltose metabolism. Plant Physiol **138:** 2280–2291

Lu Y, Sharkey TD (2004) The role of amylomaltase in maltose metabolism in the cytosol of photosynthetic cells. Planta **218:** 466–473

Lunn JE (2007) Gene families and evolution of trehalose metabolism in plants. Funct Plant Biol **34:** 550–563

Lunn JE, Feil R, Hendriks JHM, Gibon Y, Morcuende R, Osuna D, Scheible W-R, Carillo P, Hajirezaei MR, Stitt M (2006) Sugar-induced increases in trehalose 6-phosphate are correlated with redox activation of ADPglucose pyrophosphorylase and higher rates of starch synthesis in *Arabidopsis thaliana*. Biochem J **397:** 139–148

Lunn JE, Price GD, Furbank RT (1999) Cloning and expression of a prokaryotic sucrose-phosphate synthase gene from the cyanobacterium *Synechocystis* sp. PCC 6803. Plant Mol Biol **40:** 297–305

MacRae EA, Lunn JE (2006) Control of sucrose biosynthesis. *In* WC Plaxton, MT McManus, eds, Advances in Plant Research: Control of Primary Metabolism in Plants, Vol 22. Blackwell, Oxford, pp 234–257

Michalska J, Zauber H, Buchanan BB, Cejudo FJ, Geigenberger P (2009) NTRC links built-in thioredoxin to light and sucrose in regulating starch synthesis in chloroplasts and amyloplasts. Proc Natl Acad Sci USA **106:** 9908–9913

Murashige T, Skoog F (1962) A revised medium for rapid growth and bioassays with tobacco cultures. Physiol Plant **15:** 473–497

Neuhaus HE, Kruckeberg AL, Feil R, Gottlieb L, Stitt M (1989) Dosage mutants of phosphoglucose isomerase in the cytosol and chloroplasts of *Clarkia xantiana*. II. Study of the mechanisms which regulate photosynthate partitioning. Planta **178:** 110–122

Neuhaus HE, Quick WP, Siegl G, Stitt M (1990) Control of photosynthate partitioning in spinach leaves: analysis of the interaction between feedforward and feedback regulation of sucrose synthesis. Planta **181:** 583–592

Neuhaus HE, Stitt M (1990) Control analysis of photosynthate partitioning: impact of reduced activity of ADP-glucose pyrophosphorylase or plastid phosphoglucomutase on the fluxes to starch and sucrose in *Arabidopsis thaliana*. Planta **182:** 445–454

Niittylä T, Comparot-Moss S, Lue WL, Messerli G, Trevisan M, Seymour MD, Gatehouse JA, Villadsen D, Smith SM, Chen J, et al (2006) Similar protein phosphatases control starch metabolism in plants and glycogen metabolism in mammals. J Biol Chem **281:** 11815–11818

Niittylä T, Messerli G, Trevisan M, Chen J, Smith AM, Zeeman SC (2004) A previously unknown maltose transporter essential for starch degradation in leaves. Science **303:** 87–89

Pal SK, Liput M, Piques M, Ishihara H, Obata T, Martins MCM, Sulpice R, van Dongen JT, Fernie AR, Yadav UP, et al (2013) Diurnal changes of polysome loading track sucrose content in the rosette of wild-type Arabidopsis and the starchless *pgm* mutant. Plant Physiol **162:** 1246–1265

Pellny TK, Ghannoum O, Conroy JP, Schluepmann H, Smeekens S, Andralojc J, Krause KP, Goddijn O, Paul MJ (2004) Genetic modification of photosynthesis with E. coli genes for trehalose synthesis. Plant Biotechnol J **2:** 71–82

Piques M, Schulze WX, Höhne M, Usadel B, Gibon Y, Rohwer J, Stitt M (2009) Ribosome and transcript copy numbers, polysome occupancy and enzyme dynamics in Arabidopsis. Mol Syst Biol **5:** 314–330

Preiss J (1988) Biosynthesis of starch and its regulation. *In* J Preiss, ed, The Biochemistry of Plants, Vol 14. Academic Press, San Diego, pp 181–254

Pyl ET, Piques M, Ivakov A, Schulze WX, Ishihara H, Stitt M, Sulpice R (2012) Metabolism and growth in *Arabidopsis* depend on the daytime temperature but are temperature-compensated against cool nights. Plant Cell **24:** 2443–2469

Raines CA (2003) The Calvin cycle revisited. Photosynth Res **75:** 1–10

Ramon M, De Smet I, Vandesteene L, Naudts M, Leyman B, Van Dijck P, Rolland F, Beeckman T, Thevelein JM (2009) Extensive expression regulation and lack of heterologous enzymatic activity of the class II trehalose metabolism proteins from *Arabidopsis thaliana*. Plant Cell Environ **32:** 1015–1032

Ramon M, Rolland F, Thevelein JM, Van Dijck P, Leyman B (2007) ABI4 mediates the effects of exogenous trehalose on Arabidopsis growth and starch breakdown. Plant Mol Biol **63:** 195–206

Ritte G, Heydenreich M, Mahlow S, Haebel S, Kötting O, Steup M (2006) Phosphorylation of C6- and C3-positions of glucosyl residues in starch is catalysed by distinct dikinases. FEBS Lett **580:** 4872–4876

Ritte G, Lloyd JR, Eckermann N, Rottmann A, Kossmann J, Steup M (2002) The starch-related R1 protein is an α-glucan, water dikinase. Proc Natl Acad Sci USA **99:** 7166–7171

Santelia D, Kötting O, Seung D, Schubert M, Thalmann M, Bischof S, Meekins DA, Lutz A, Patron N, Gentry MS, et al (2011) The phosphoglucan phosphatase like sex Four2 dephosphorylates starch at the C3-position in *Arabidopsis*. Plant Cell **23:** 4096–4111

Schluepmann H, Pellny T, van Dijken A, Smeekens S, Paul M (2003) Trehalose 6-phosphate is indispensable for carbohydrate utilization and growth in *Arabidopsis thaliana*. Proc Natl Acad Sci USA **100:** 6849–6854

Scialdone A, Mugford ST, Feike D, Skeffington A, Borrill P, Graf A, Smith AM, Howard M (2013) Arabidopsis plants perform arithmetic division to prevent starvation at night. eLife **2:** e00669

Scott P, Lange AJ, Kruger NJ (2000) Photosynthetic carbon metabolism in leaves of transgenic tobacco (*Nicotiana tabacum* L.) containing decreased amounts of fructose 2,6-bisphosphate. Planta **211:** 864–873

Smith AM, Stitt M (2007) Coordination of carbon supply and plant growth. Plant Cell Environ **30:** 1126–1149

Smith SM, Fulton DC, Chia T, Thorneycroft D, Chapple A, Dunstan H, Hylton C, Zeeman SC, Smith AM (2004) Diurnal changes in the transcriptome encoding enzymes of starch metabolism provide evidence for both transcriptional and posttranscriptional regulation of starch metabolism in Arabidopsis leaves. Plant Physiol **136:** 2687–2699

Steup M (1990) Starch degrading enzymes. *In* PJ Lea, ed, Methods in Plant Biochemistry, Vol 3. Academic Press, London, pp 103–128

Stitt M, Gibon Y, Lunn JE, Piques M (2007) Multilevel genomics analysis of carbon signaling during diurnal cycles: balancing supply and utilization by responding to changes in the nonlimiting range. Funct Plant Biol **34:** 526–549

Stitt M, Lilley RM, Gerhardt R, Heldt HW (1989) Determination of metabolite levels in specific cells and subcellular compartments of plant leaves. Methods Enzymol **174:** 518–552

Stitt M, Lunn J, Usadel B (2010) Arabidopsis and primary photosynthetic metabolism: more than the icing on the cake. Plant J **61:** 1067–1091

Stitt M, Sonnewald U (1995) Regulation of metabolism in transgenic plants. Annu Rev Plant Physiol Plant Mol Biol **46:** 341–368

Stitt M, Wilke I, Feil R, Heidt HW (1988) Coarse control of sucrose-phosphate synthase in leaves: alterations of the kinetic properties in response to the rate of photosynthesis and the accumulation of sucrose. Planta **174:** 217–230

Stitt M, Zeeman SC (2012) Starch turnover: pathways, regulation and role in growth. Curr Opin Plant Biol **15:** 282–292

Strand A, Zrenner R, Stitt M, Gardestrom P (2000) Antisense inhibition of two key enzymes in the sucrose biosynthesis pathway, cytosolic fructose bisphosphatase and sucrose phosphate synthase, has different consequences for photosynthetic carbon metabolism in transgenic *Arabidopsis thaliana*. Plant J **23:** 751–770

Streb S, Eicke S, Zeeman SC (2012) The simultaneous abolition of three starch hydrolases blocks transient starch breakdown in Arabidopsis. J Biol Chem **287:** 41745–41756

Szecowka M, Heise R, Tohge T, Nunes-Nesi A, Vosloh D, Huege J, Feil R, Lunn J, Nikoloski Z, Stitt M, et al (2013) Metabolic fluxes in an illuminated *Arabidopsis* rosette. Plant Cell **25:** 694–714

Tagliabracci VS, Roach PJ (2010) Insights into the mechanism of polysaccharide dephosphorylation by a glucan phosphatase. Proc Natl Acad Sci USA **107:** 15312–15313

Tanz SK, Castleden I, Hooper CM, Vacher M, Small I, Millar AH (2012) SUBA3: a database for integrating experimentation and prediction to define the SUBcellular location of proteins in Arabidopsis. Nucleic Acids Res **41:** D1185–D1191

Tiessen A, Hendriks JHM, Stitt M, Branscheid A, Gibon Y, Farré EM, Geigenberger P (2002) Starch synthesis in potato tubers is regulated by post-translational redox modification of ADP-glucose pyrophosphorylase: a novel regulatory mechanism linking starch synthesis to the sucrose supply. Plant Cell **14:** 2191–2213

Usadel B, Bläsing OE, Gibon Y, Retzlaff K, Höhne M, Günther M, Stitt M (2008) Global transcript levels respond to small changes of the carbon status during progressive exhaustion of carbohydrates in Arabidopsis rosettes. Plant Physiol **146:** 1834–1861

Valerio C, Costa A, Marri L, Issakidis-Bourguet E, Pupillo P, Trost P, Sparla F (2011) Thioredoxin-regulated beta-amylase (BAM1) triggers diurnal starch degradation in guard cells, and in mesophyll cells under osmotic stress. J Exp Bot **62:** 545–555

Vandesteene L, López-Galvis L, Vanneste K, Feil R, Maere S, Lammens W, Rolland F, Lunn JE, Avonce N, Beeckman T, et al (2012) Expansive evolution of the trehalose-6-phosphate phosphatase gene family in Arabidopsis. Plant Physiol **160:** 884–896

Van Dijck P, Mascorro-Gallardo JO, De Bus M, Royackers K, Iturriaga G, Thevelein JM (2002) Truncation of *Arabidopsis thaliana* and *Selaginella lepidophylla* trehalose-6-phosphate synthase unlocks high catalytic activity and supports high trehalose levels on expression in yeast. Biochem J **366:** 63–71

Weber A, Servaites JC, Geiger DR, Kofler H, Hille D, Gröner F, Hebbeker U, Flügge UI (2000) Identification, purification, and molecular cloning of a putative plastidic glucose translocator. Plant Cell **12:** 787–802

Weise SE, Schrader SM, Kleinbeck KR, Sharkey TD (2006) Carbon balance and circadian regulation of hydrolytic and phosphorolytic breakdown of transitory starch. Plant Physiol **141:** 879–886

Weise SE, Weber APM, Sharkey TD (2004) Maltose is the major form of carbon exported from the chloroplast at night. Planta **218:** 474–482

Wingler A, Delatte TL, O'Hara LE, Primavesi LF, Jhurreea D, Paul MJ, Schluepmann H (2012) Trehalose 6-phosphate is required for the onset of leaf senescence associated with high carbon availability. Plant Physiol **158:** 1241–1251

Wingler A, Fritzius T, Wiemken A, Boller T, Aeschbacher RA (2000) Trehalose induces the ADP-glucose pyrophosphorylase gene, *ApL3*, and starch synthesis in Arabidopsis. Plant Physiol **124:** 105–114

Winter H, Robinson DG, Heldt HW (1993) Subcellular volumes and metabolite concentrations in barley leaves. Planta **191:** 180–190

Winter H, Robinson DG, Heldt HW (1994) Subcellular volumes and metabolite concentrations in spinach leaves. Planta **193:** 530–535

Worby CA, Gentry MS, Dixon JE (2006) Laforin, a dual specificity phosphatase that dephosphorylates complex carbohydrates. J Biol Chem **281:** 30412–30418

Wuyts N, Palauqui JC, Conejero G, Verdeil JL, Granier C, Massonnet C (2010) High-contrast three-dimensional imaging of the Arabidopsis leaf enables the analysis of cell dimensions in the epidermis and mesophyll. Plant Methods **6:** 17–30

Yazdanbakhsh N, Sulpice R, Graf A, Stitt M, Fisahn J (2011) Circadian control of root elongation and C partitioning in *Arabidopsis thaliana*. Plant Cell Environ **34:** 877–894

Zeeman SC, Kossmann J, Smith AM (2010) Starch: its metabolism, evolution, and biotechnological modification in plants. Annu Rev Plant Biol **61:** 15.1–15.26

Zeeman SC, Tiessen A, Pilling E, Kato KL, Donald AM, Smith AM (2002) Starch synthesis in Arabidopsis: granule synthesis, composition, and structure. Plant Physiol **129:** 516–529

Zhang Y, Primavesi LF, Jhurreea D, Andralojc PJ, Mitchell RAC, Powers SJ, Schluepmann H, Delatte T, Wingler A, Paul MJ (2009) Inhibition of SNF1 related protein kinase1 activity and regulation of metabolic pathways by trehalose-6-phosphate. Plant Physiol **149:** 1860–1871

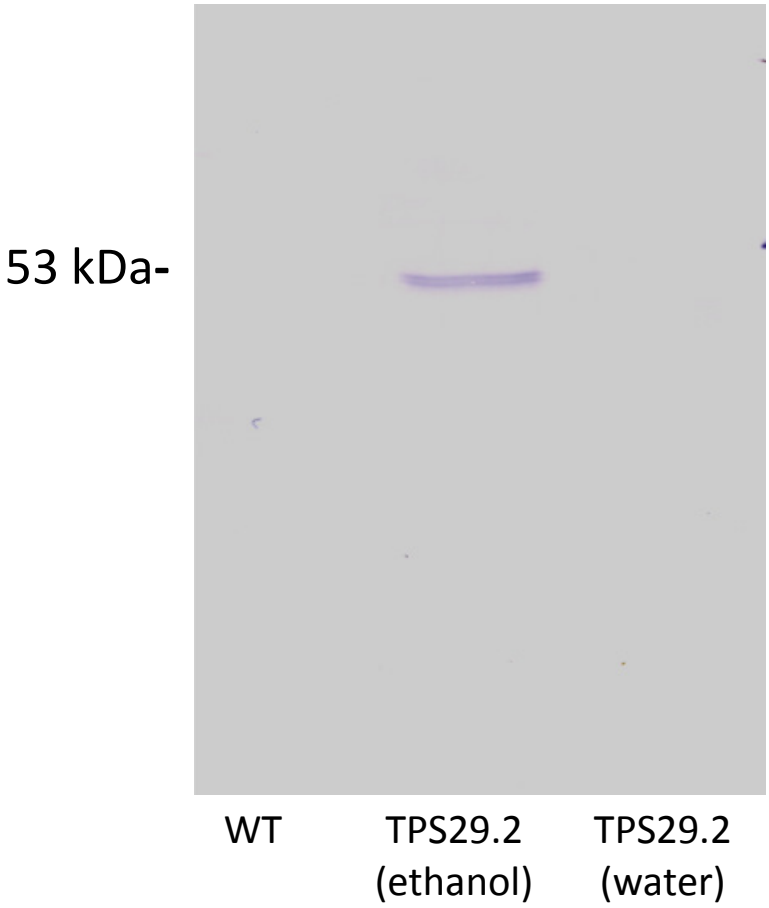

Supplemental Figure S1. Inducible expression of *E. coli* otsA (TPS) in Arabidopsis. Immunoblot of leaf proteins (20 µg per lane) extracted from: (i) WT Col-0, (ii) TPS29.2 sprayed with ethanol and (iii) TPS29.2 sprayed with water, probed with antibody raised against the *E. coli* otsA (TPS) protein. Leaves were harvested 24 h after spraying.

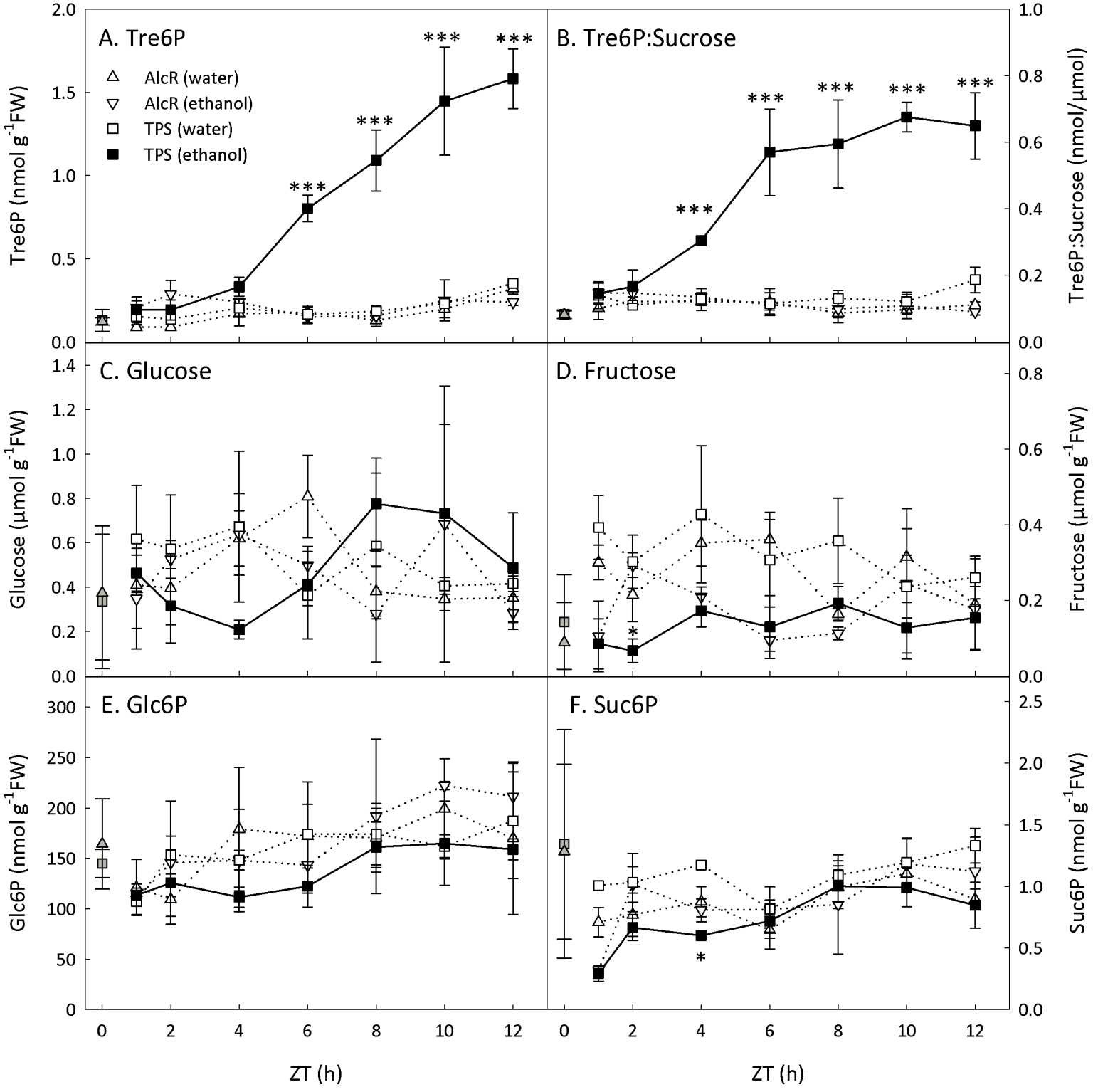

Supplemental Figure S2. Effect of TPS over-expression on the metabolite content of Arabidopsis rosettes during the day.

Ethanol-inducible TPS line 29.2 (TPS) and plants expressing the ethanol-binding transcription factor (AlcR) were grown in soil with a 12-h photoperiod. Four-week-old plants were sprayed with water or 2% (v/v) ethanol at the beginning of the day and harvested at 1 or 2-h intervals after spraying for determination of: (A) Tre6P, (B) Tre6P:sucrose ratio (C) glucose, (D) fructose, (E) Glc6P, and (F) Suc6P. Grey symbols at t=0 represent unsprayed AlcR (grey triangle) or TPS (grey square) plants. Data are mean ± S.D. (n = 3). Significant differences (one-way ANOVA, Holm-Sidak test) between the ethanol-sprayed TPS line and the three controls – AlcR (sprayed with water or ethanol) and TPS (water) – are indicated by asterisks: *P<0.05, **P<0.01, ***P<0.001.

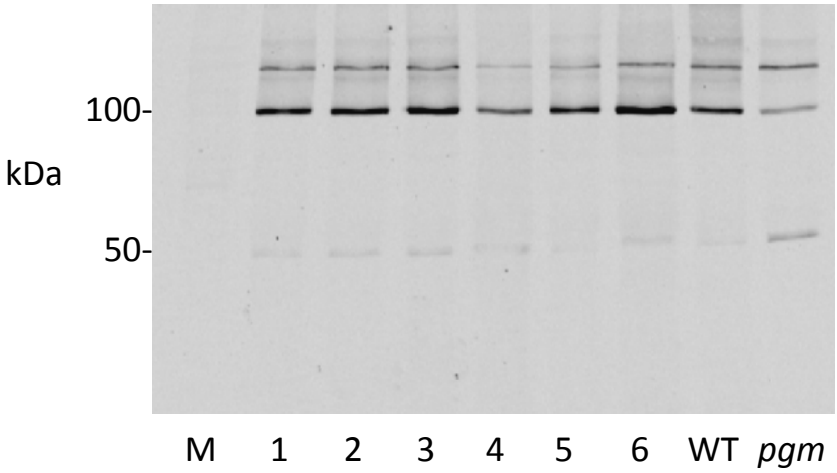

Supplemental Figure S3. Immunoblotting of the APS1 protein in Arabidopsis leaf extracts to determine the redox status of AGPase.

Arabidopsis rosette leaves were extracted in trichloroacetic acid to maintain the redox status of the APS1 protein and subjected to immunoblotting after SDS-PAGE under non-reducing conditions as described in Hendriks et al. (2003). Quantitative detection of APS1 protein was performed using an Odyssey infrared imaging system as described in Hädrich et al. (2011). Extracts from WT Col-0 and the *pgm* mutant were included as controls on each gel to allow correction for variation between gels. The redox status of AGPase is expressed as the percentage of total APS1 protein present as the 50-kDa monomer. The values were normalised by linear scaling to the average values for the WT Col-0 and *pgm* values across all the blots. (M = molecular weight marker)

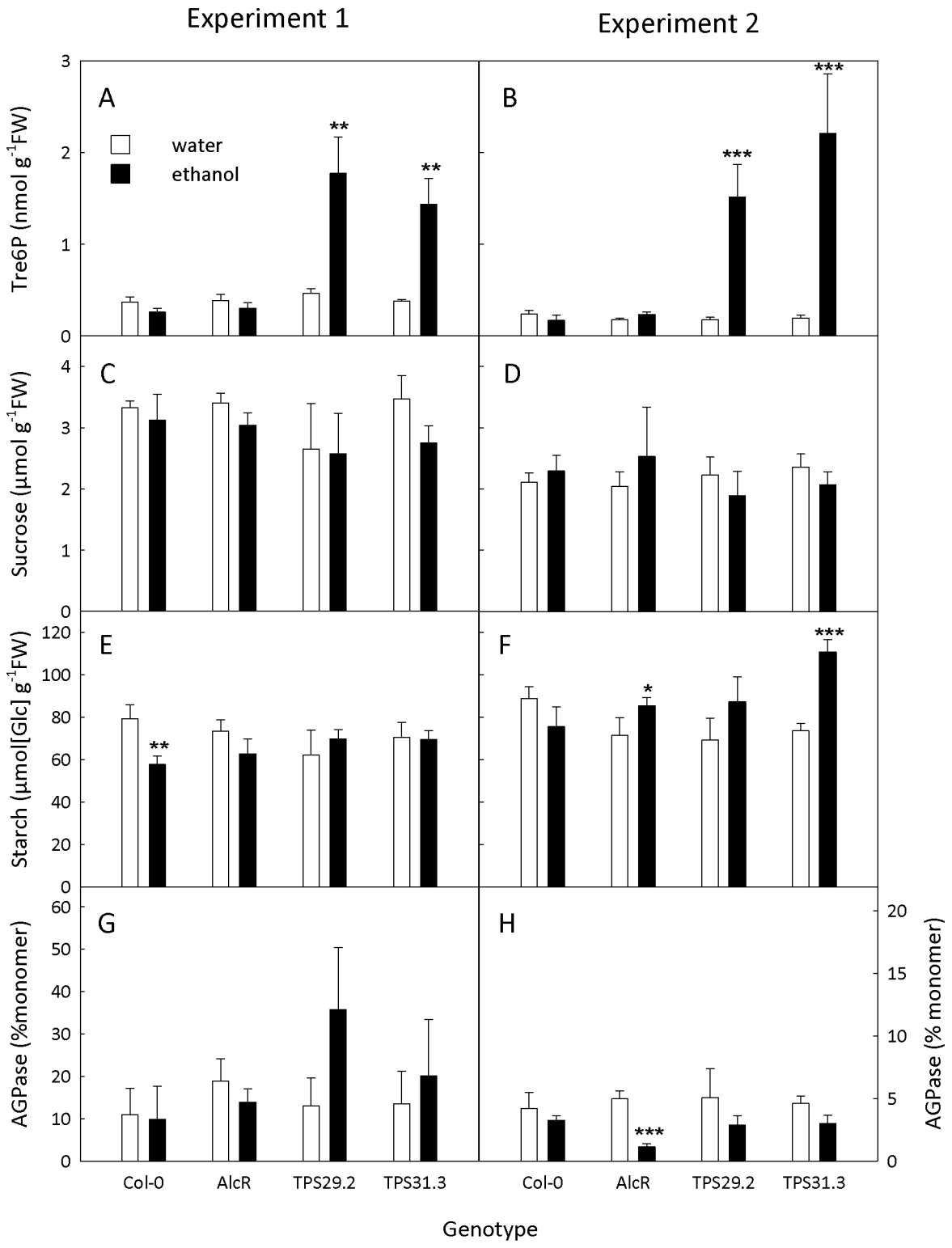

Supplemental Figure S4. Effect of TPS over-expression on the metabolite content of Arabidopsis rosettes during the day.

Ethanol-inducible TPS plants (TPS29.2 and TPS31.3) were grown in soil with a 12-h photoperiod. Wild-type (Col-0) and plants expressing the AlcR ethanol-binding transcription factor (AlcR) were grown as controls. Four-week-old plants were sprayed with water (white bars) or 2% (v/v) ethanol (black bars) at the beginning of the day. Data are shown from two independent experiments: Expt. 1 (left column) and Expt. 2 (right column). Pools of ten rosettes were harvested 12 h later at the end of the day for determination of: (A-B) Tre6P; (C-D) sucrose; (E-F) starch; (G-H) oligomeric status of ADP-glucose pyrophosphorylase (n.b. different *y*-axis scales in G and H); (I) trehalose (Expt. 1 only); (J-K) glucose; (L-M) fructose; and (N-O) starch/sucrose (based on µmol[hexose equivalents] g^{-1}FW). Data are mean ± S.D. (n=3, Expt. 1 or n=4, Expt. 2). Significant differences between ethanol and water treated plants from the same genotype are indicated by asterisks (Student's t-test) *P<0.05, **P<0.01, ***P<0.001.

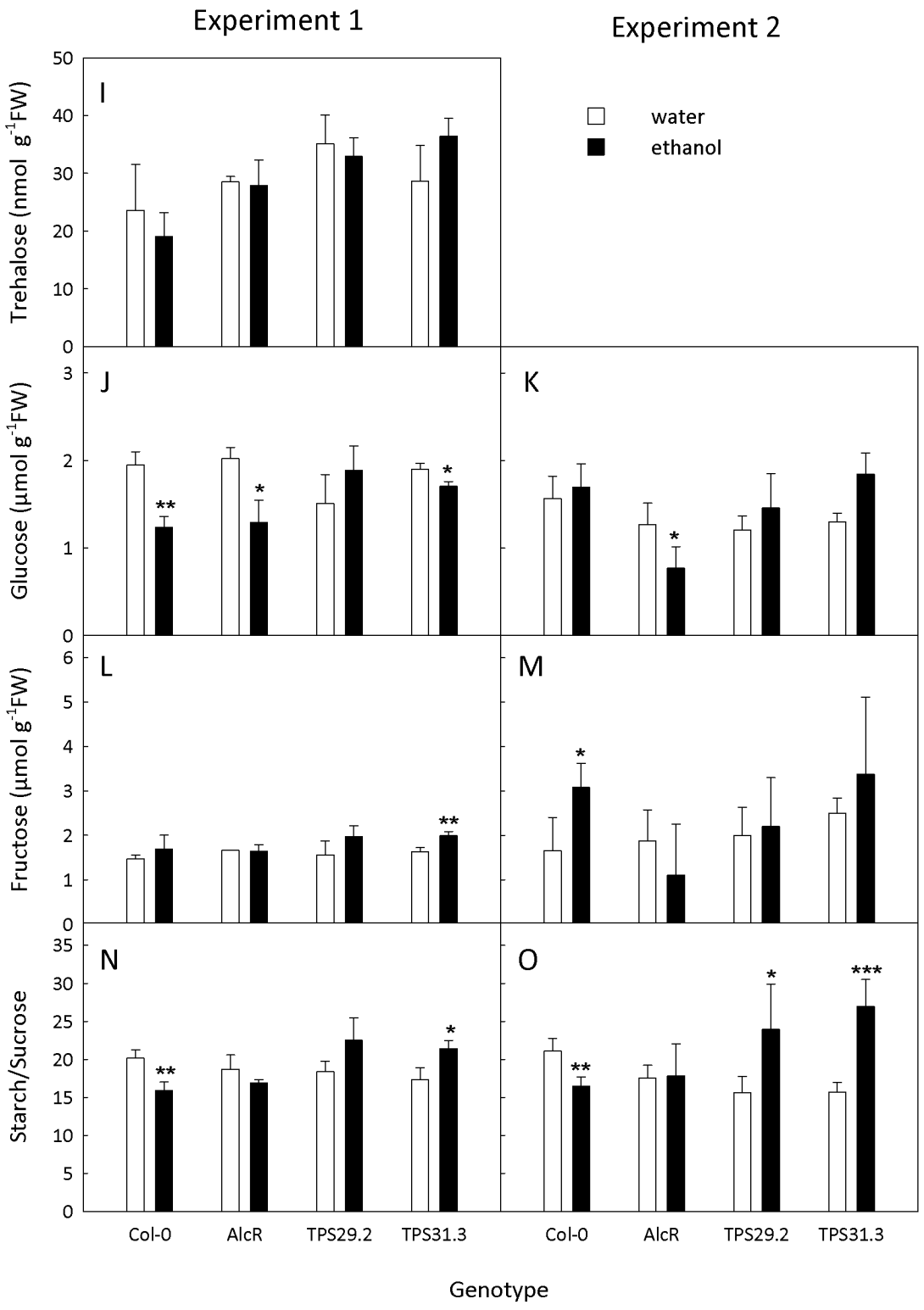

Supplemental Figure S4. Effect of TPS over-expression on the metabolite content of Arabidopsis rosettes during the day.

Ethanol-inducible TPS plants (TPS29.2 and TPS31.3) were grown in soil with a 12-h photoperiod. Wild-type (Col-0) and plants expressing the AlcR ethanol-binding transcription factor (AlcR) were grown as controls. Four-week-old plants were sprayed with water (white bars) or 2% (v/v) ethanol (black bars) at the beginning of the day. Data are shown from two independent experiments: Expt. 1 (left column) and Expt. 2 (right column). Pools of ten rosettes were harvested 12 h later at the end of the day for determination of: (A-B) Tre6P; (C-D) sucrose; (E-F) starch; (G-H) oligomeric status of ADP-glucose pyrophosphorylase (n.b. different *y*-axis scales in G and H); (I) trehalose (Expt. 1 only); (J-K) glucose; (L-M) fructose; and (N-O) starch/sucrose (based on µmol[hexose equivalents] g^{-1}FW). Data are mean ± S.D. (n=3, Expt. 1 or n=4, Expt. 2). Significant differences between ethanol and water treated plants from the same genotype are indicated by asterisks (Student's t-test) *P<0.05, **P<0.01, ***P<0.001.

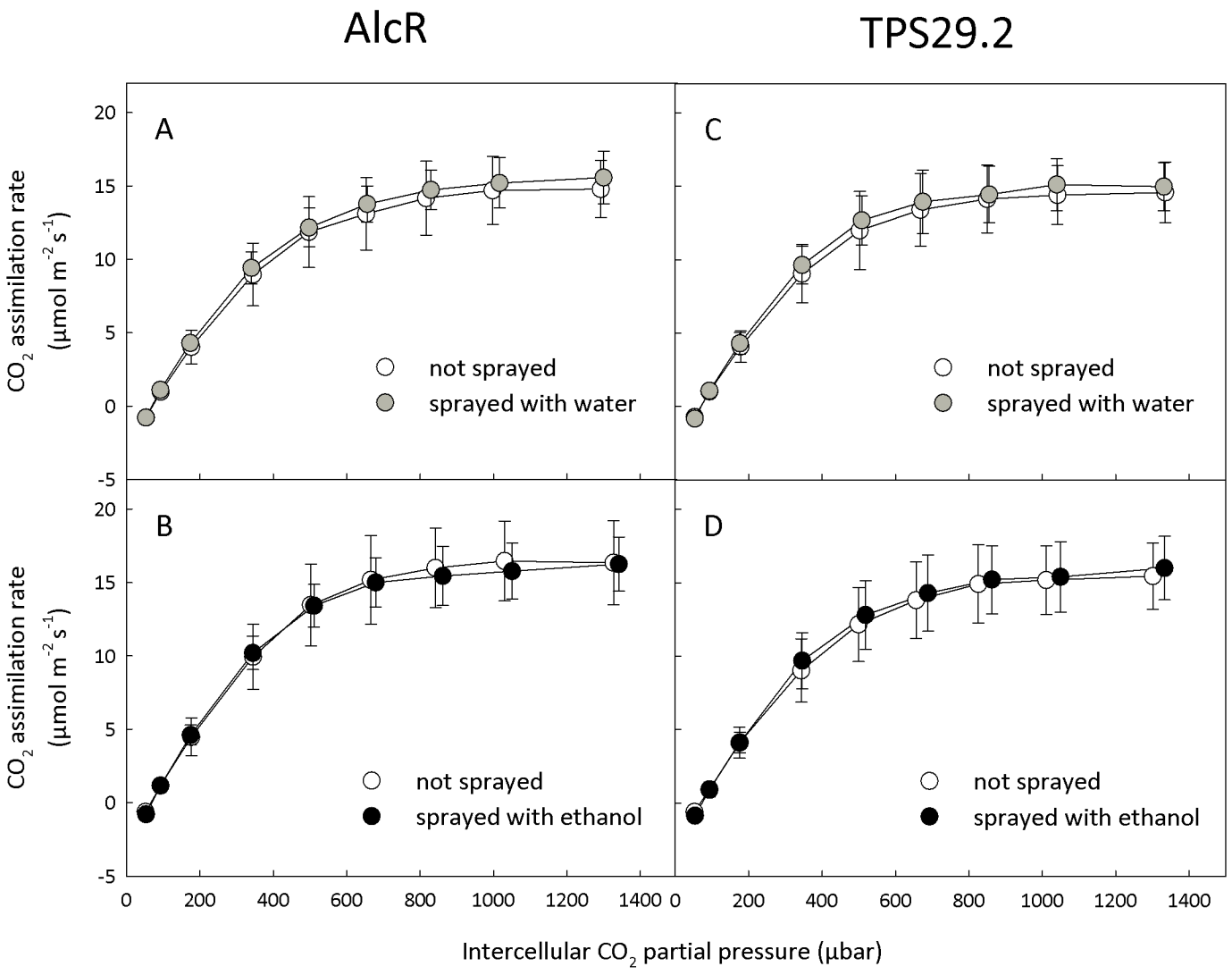

Supplemental Figure S5. Effect of induced changes in Tre6P on photosynthetic CO_2 assimilation in Arabidopsis rosettes.

AlcR (A-B) and TPS29.2 (C-D) plants were grown in soil with a 12-h photoperiod. Net CO_2 assimilation rates at different intercellular CO_2 concentrations were measured in intact rosettes of 3 to 4-week-old plants by infra-red gas analysis using a Li-Cor LI-6400XT Photosynthesis System (Li-Cor, Lincoln NE). The plants were then sprayed with either water (A,C) or 2 % (v/v) ethanol (B,D) at the end of the day, and net CO_2 assimilation rates were measured the following day (12-22 h after spraying). Values are mean ± S.D. (n = 7 individual plants).

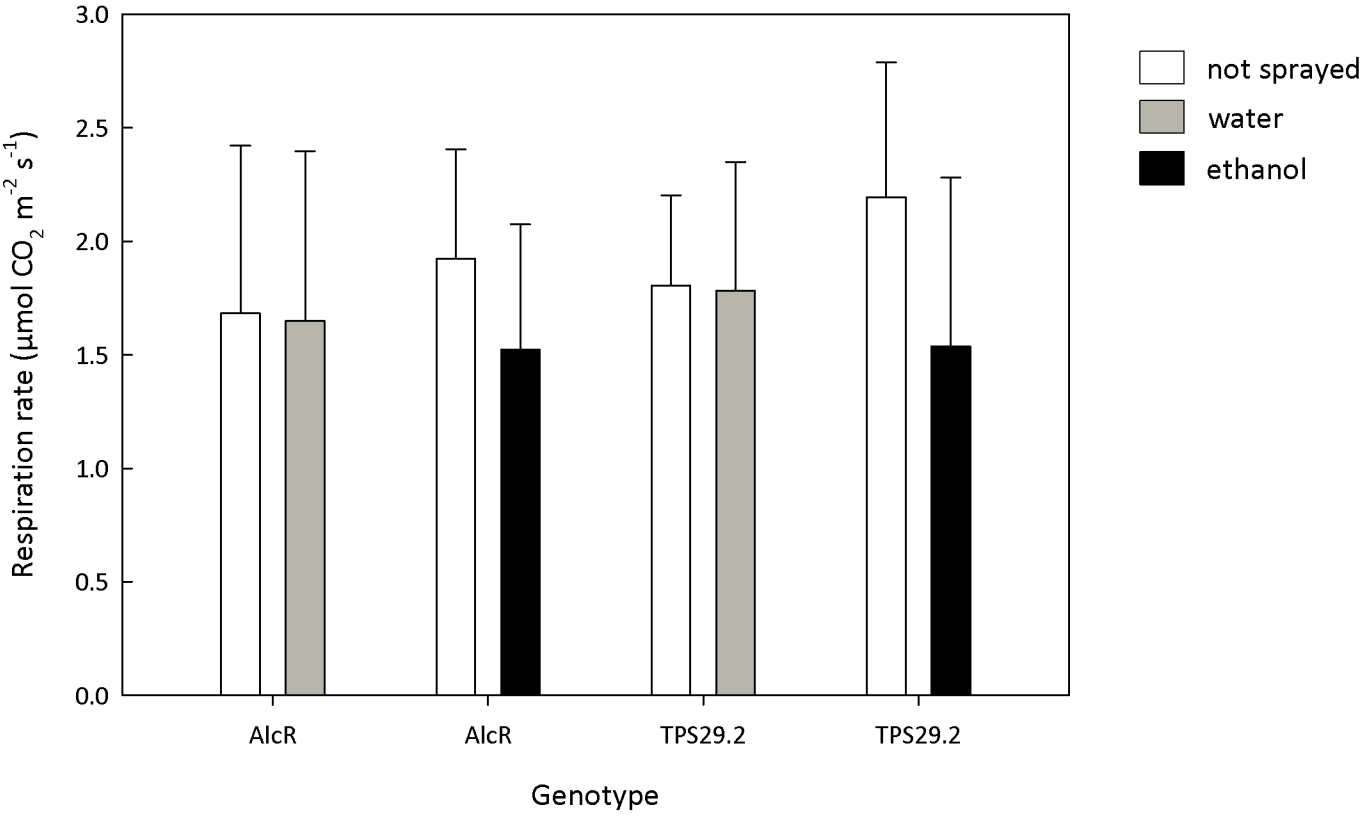

Supplemental Figure S6. Effect of induced changes in Tre6P on dark respiration in Arabidopsis rosettes.

AlcR and TPS29.2 plants were grown in soil with a 12-h photoperiod. Dark respiration rates were measured in intact rosettes of unsprayed (white bars) 3 to 4-week-old plants by infra-red gas analysis using a Li-Cor LI-6400XT Photosynthesis System (Li-Cor, Lincoln NE). The plants were then sprayed with either water (grey bars) or 2 % (v/v) ethanol (black bars) at the end of the day, and dark respiration rates were measured the following day (12-22 h after spraying). Values are mean ± S.D. (n = 7 individual plants). There were no significant differences between genotypes or treatments according to one-way ANOVA.

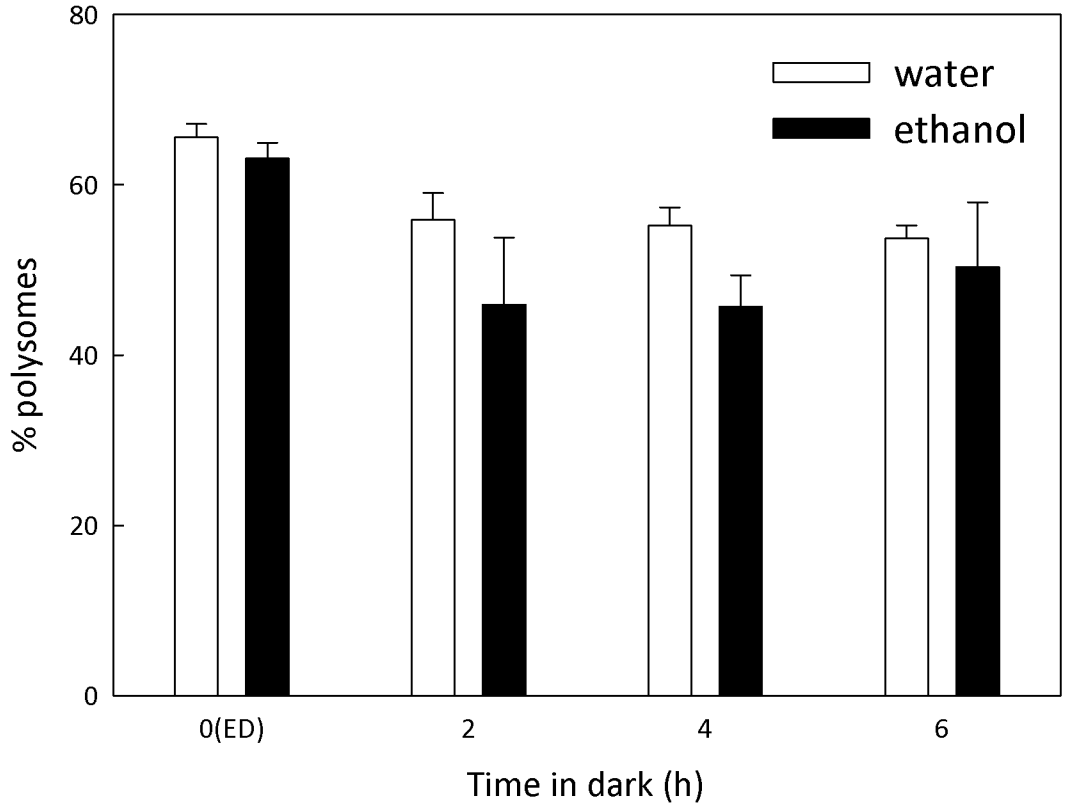

Supplemental Figure S7. Effect of Tre6P on polysome loading in Arabidopsis rosettes at night.

Ethanol-inducible TPS29.2 plants were grown in soil with a 12-h photoperiod. Four-week-old plants were sprayed with water or 2% (v/v) ethanol at the end of the day. Pools of five rosettes were harvested at the end of the day and at 2-h intervals through the night (samples are the same as those shown in Fig. 3A-D). Polysome loading was determined by sucrose density gradient centrifugation. Data are mean ± S.D. (n=3). There were no significant differences between the water and ethanol treated plants at the same time point according to Student's t-test.

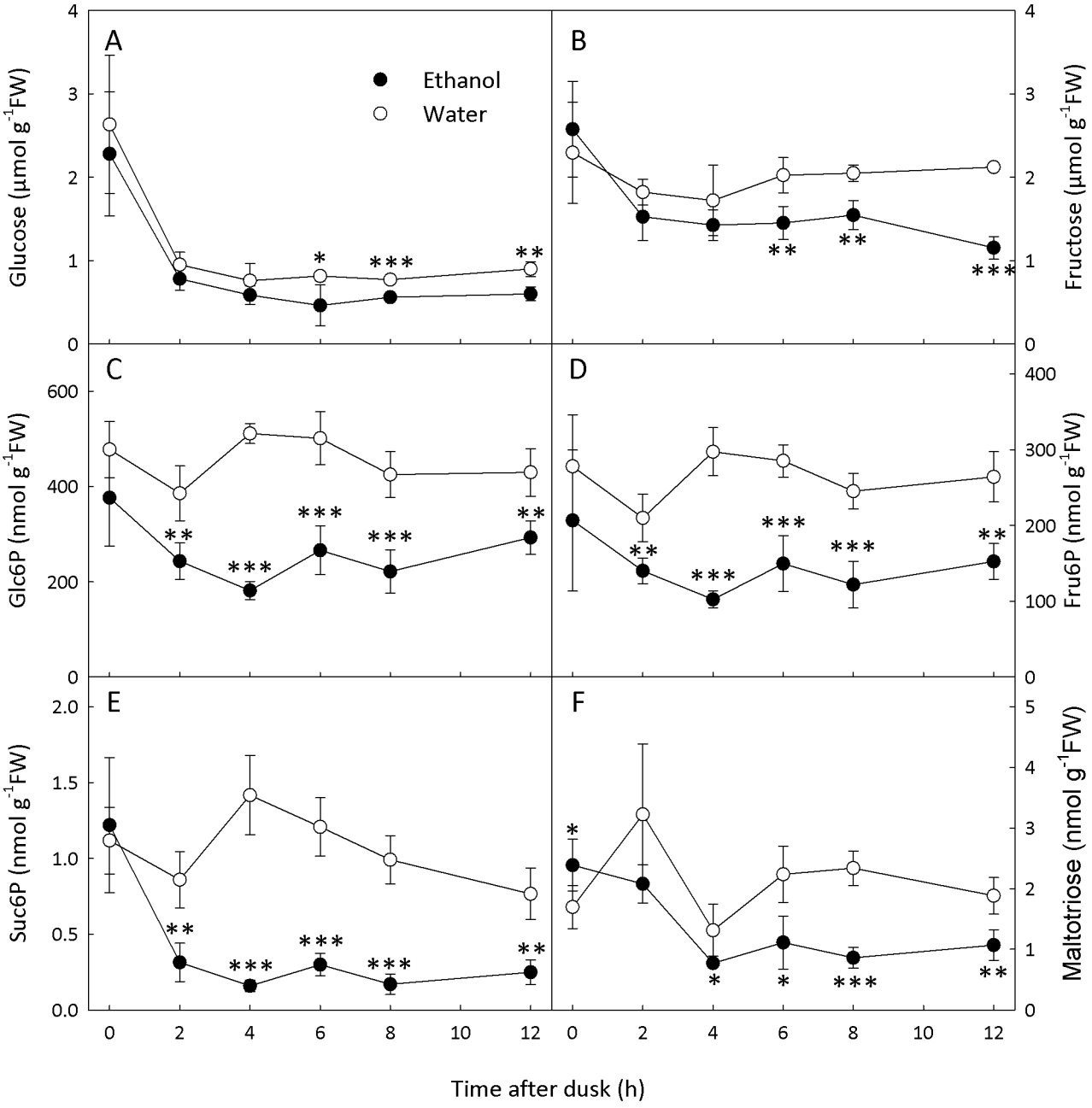

Supplemental Figure S8. Effect of inducing Tre6P synthesis at the end of the day on metabolite levels during the following night.

Ethanol-inducible TPS29.2 plants were grown in soil with a 12-h photoperiod. Four-week-old plants were sprayed with water (open symbols) or 2% (v/v) ethanol (closed symbols) at the end of the day. Pools of five rosettes were harvested at the end of the day and at 2 or 4 h intervals through the night for determination of: (A) glucose, (B) fructose, (C) Glc6P, (D) Fru6P, (E) Suc6P and (F) maltotriose. Data are mean ± S.D. (n=3). Significant differences between the water and ethanol treated plants at the same time point are indicated by asterisks (Student's t-test) *P<0.05, **P<0.01, ***P<0.001.

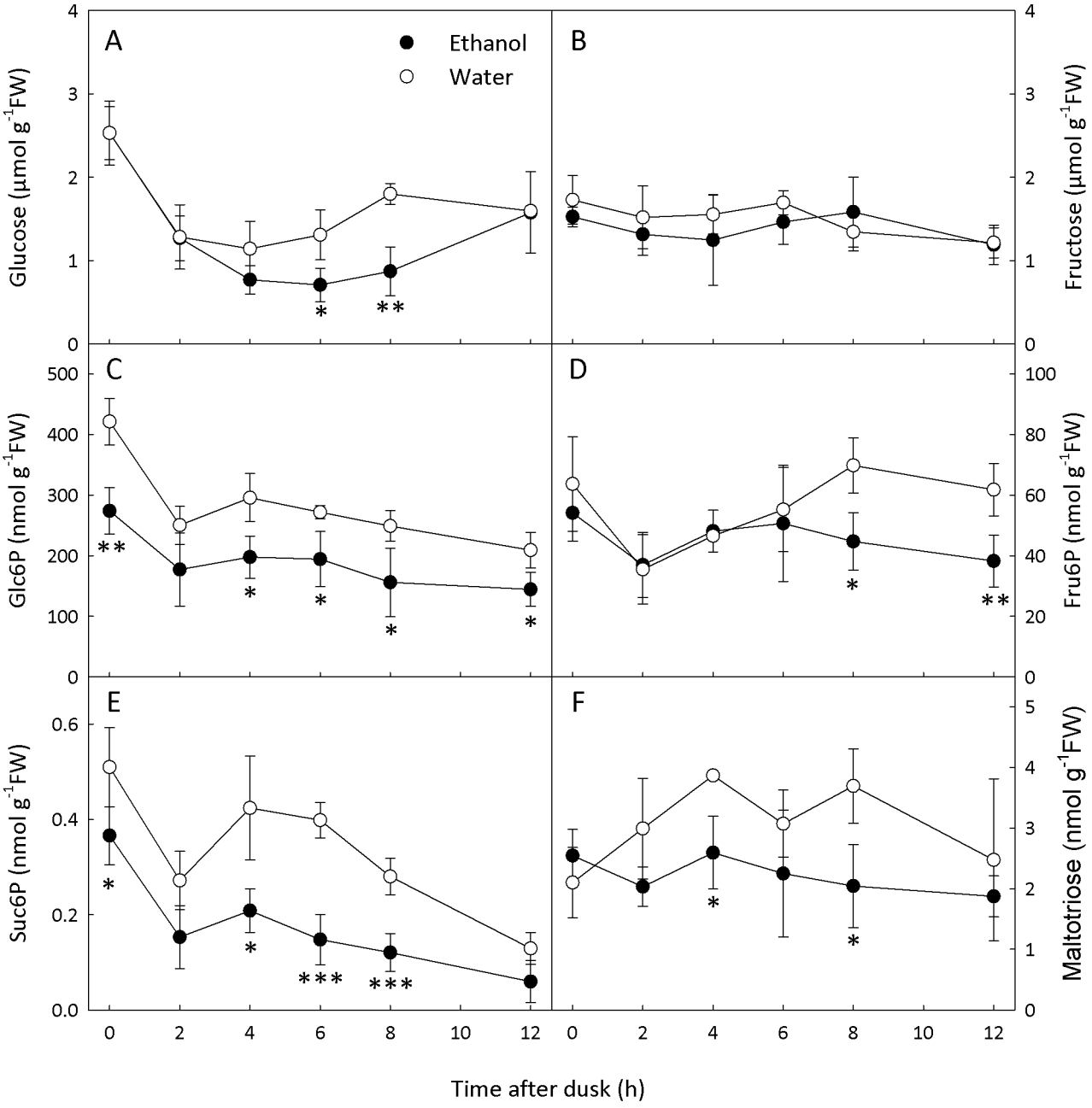

Supplemental Figure S9. Effect of inducing Tre6P synthesis in the middle of the day on metabolite levels during the following night.

Ethanol-inducible TPS29.2 plants were grown in soil with a 12-h photoperiod. Four-week-old plants were sprayed with water (open symbols) or 2% (v/v) ethanol (closed symbols) 6 h before the end of the day. Pools of five rosettes were harvested at the end of the day and at 2 or 4 h intervals through the night for determination of: (A) glucose, (B) fructose, (C) Glc6P, (D) Fru6P, (E) Suc6P and (F) maltotriose. Data are mean ± S.D. (n=3). Significant differencesbetween ethanol and water treated plants at the same time point are indicated by asterisks (Student's t-test) *P<0.05, **P<0.01, ***P<0.001.

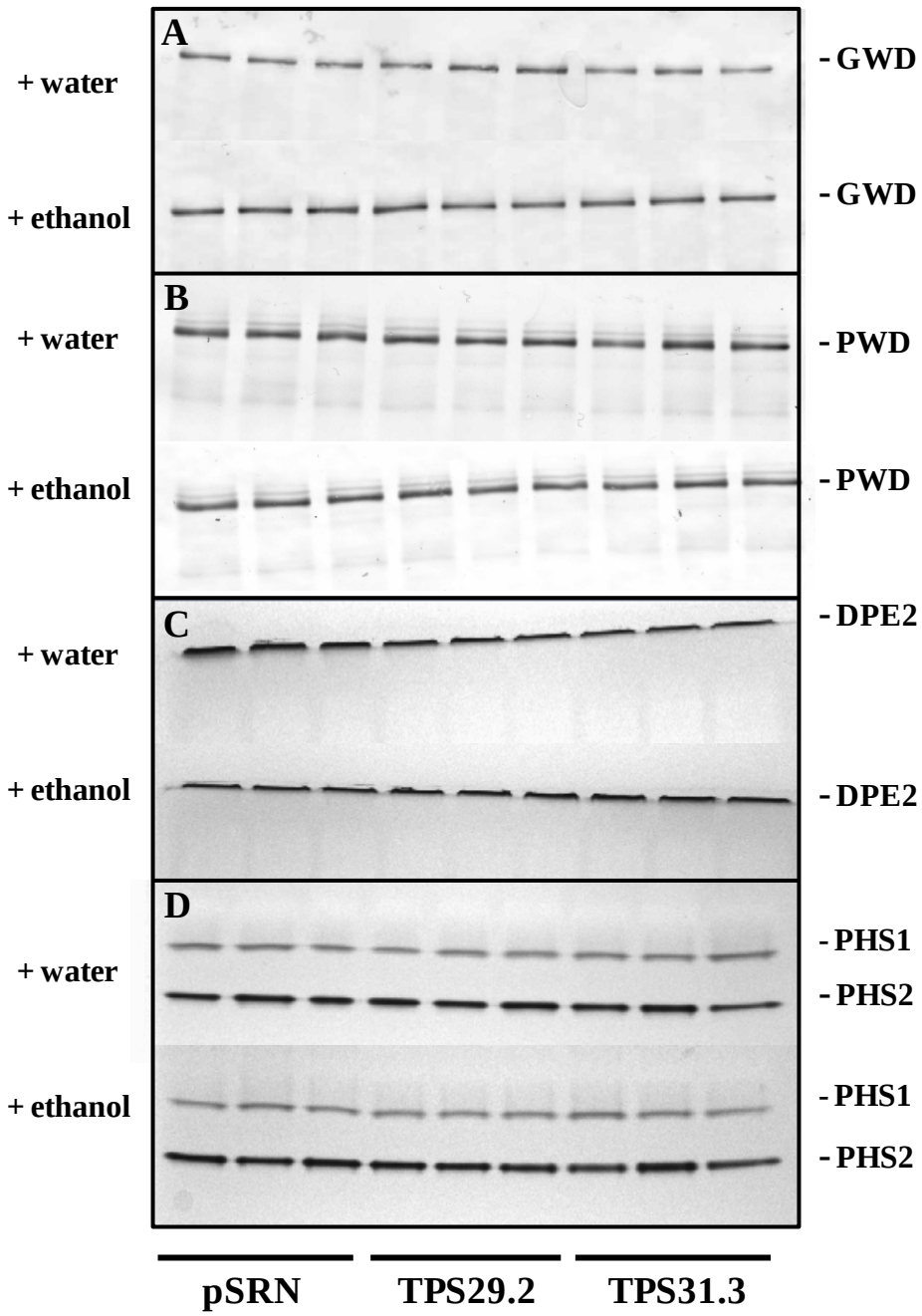

Supplemental Figure S10. Effect of induced changes in Tre6P on enzymes involved in starch degradation in *A. thaliana* rosettes. Ethanol-inducible TPS lines (TPS29.2 and TPS31.3) and AlcR (negative control) were grown in soil with a 12-h photoperiod. Four-week-old plants were sprayed at the end of the day with either water or 2 % (v/v) ethanol and harvested at the end of the night. In each section, the upper and lower panels show data from water and ethanol sprayed plants, respectively. Protein abundance of (A) glucan, water dikinase (GWD) and (B) phosphoglucan, water dikinase (PWD) was determined by immunoblotting (25 µg protein per lane). Catalytic activities of (C) cytosolic disproportionating enzyme (DPE2), and (D) plastidial glucan phosphorylase (PHS1) and cytosolic glucan phosphorylase (PHS2) were compared by *in situ* activity staining following gel electrophoresis under non-denaturing conditions. Three independent biological replicates are shown for each line.

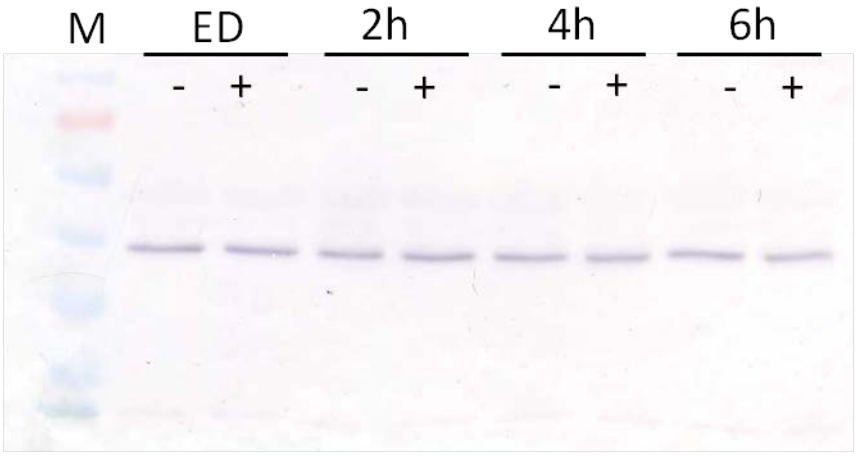

Supplemental Figure S11. Effect of induced changes in Tre6P on the SEX4 phosphoglucan phosphatase in *A. thaliana* rosettes. Immunoblot showing the abundance of SEX4 (phosphoglucan phosphatase) protein in leaf extracts from inducible TPS29.2 plants sprayed with water (-) or 2% (v/v) ethanol (+) 6 h before the end of the day (ED) and harvested at 2-h intervals during the night (25 µg protein per lane). M, prestained protein molecular weight markers.

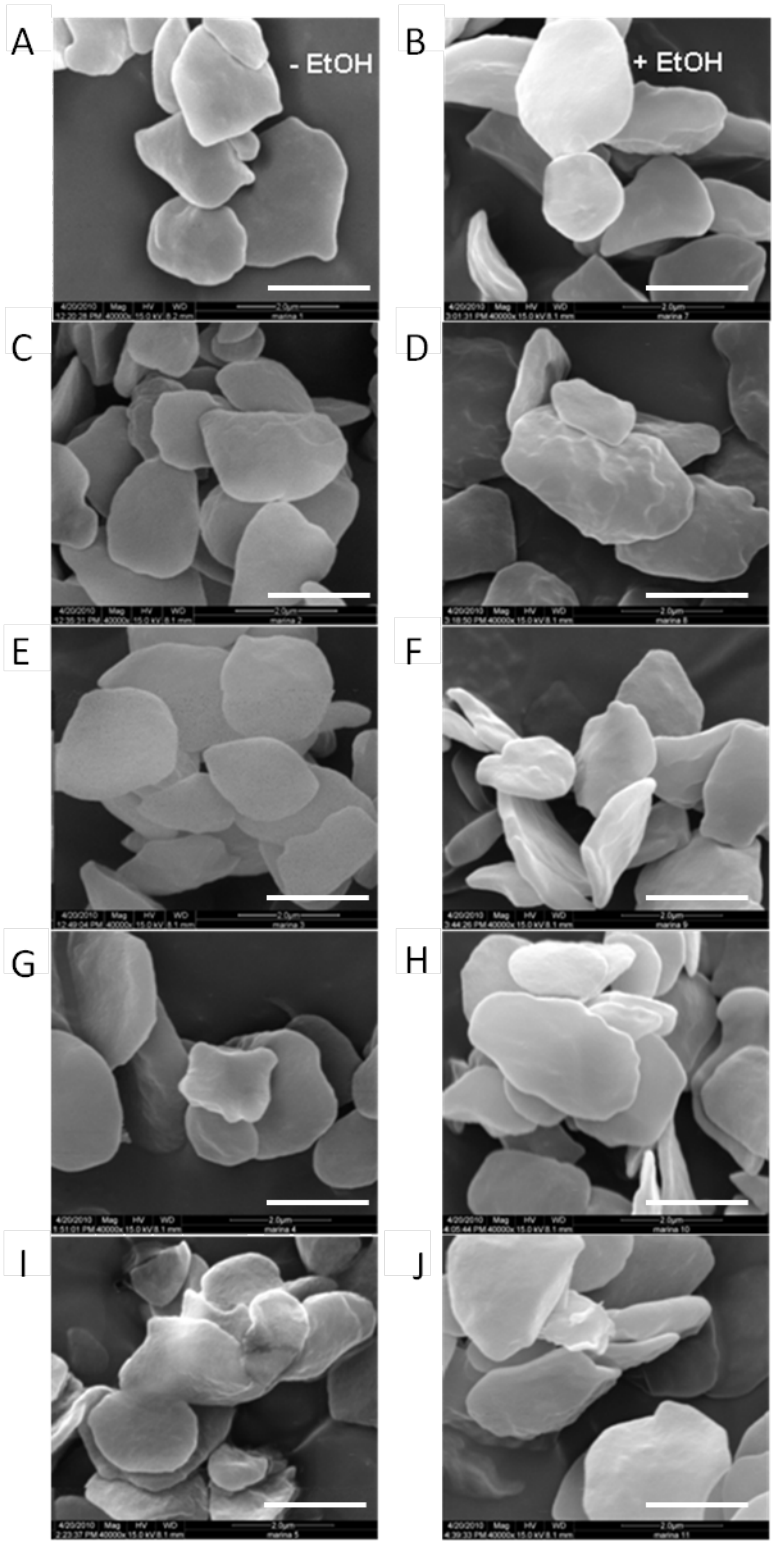

Supplemental Figure S12. Scanning electron micrographs of starch granules isolated from induced and non-induced TPS29.2 plants. Inducible TPS29.2 plants were sprayed with water (A,C,E,G,I) or 2% (v/v) ethanol (B,D,F,H,J) 6 h before the end of the day (ED), and harvested at the ED (A,B) and at 2 h (C,D), 4 h (E,F), 6 h (G,H) and 8 h (I,J) into the night. Starch granules were isolated, coated with gold, and imaged by scanning electron microscopy. Bar = 2 µm.

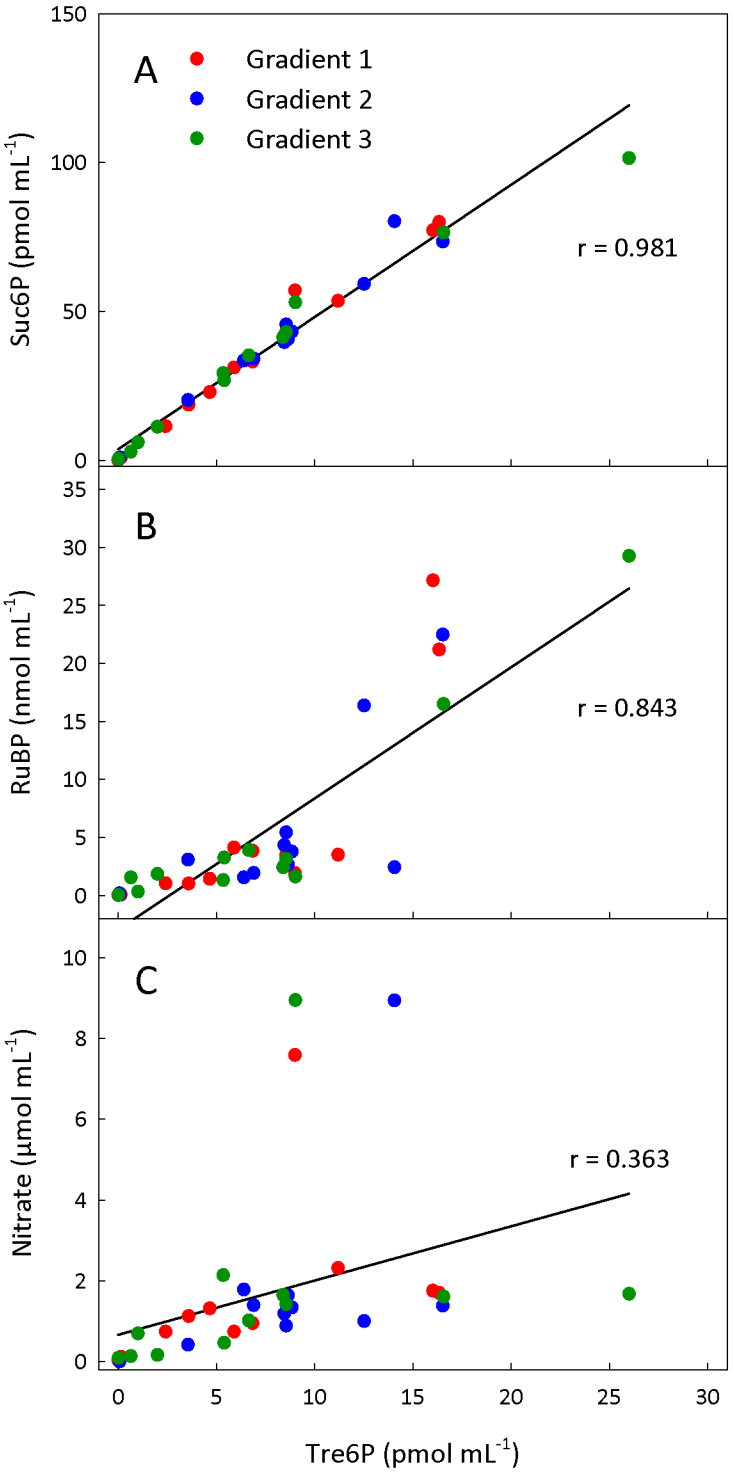

Supplemental Figure S13. Subcellular compartmentation of Tre6P in Arabidopsis rosettes. Wild type Arabidopsis Col-0 plants were grown in short day (8 h light/16 h night) conditions (see Table 1, Experiment 1). Rosettes were harvested from 5-week-old plants between 4-5 h into the light period, frozen and ground to a fine powder in liquid N_2, lyophilized and fractionation by centrifugation on non-aqueous density gradients. The amounts of Tre6P in each fraction are compared with the amounts of: (A) Suc6P (metabolite marker for the cytosol), (B) RuBP (chloroplast) and (C) nitrate (vacuole). Data are individual measurements from three gradients derived from the same batch of leaf material. Pearson's correlation coefficient (r) is shown for each pairwise comparison.

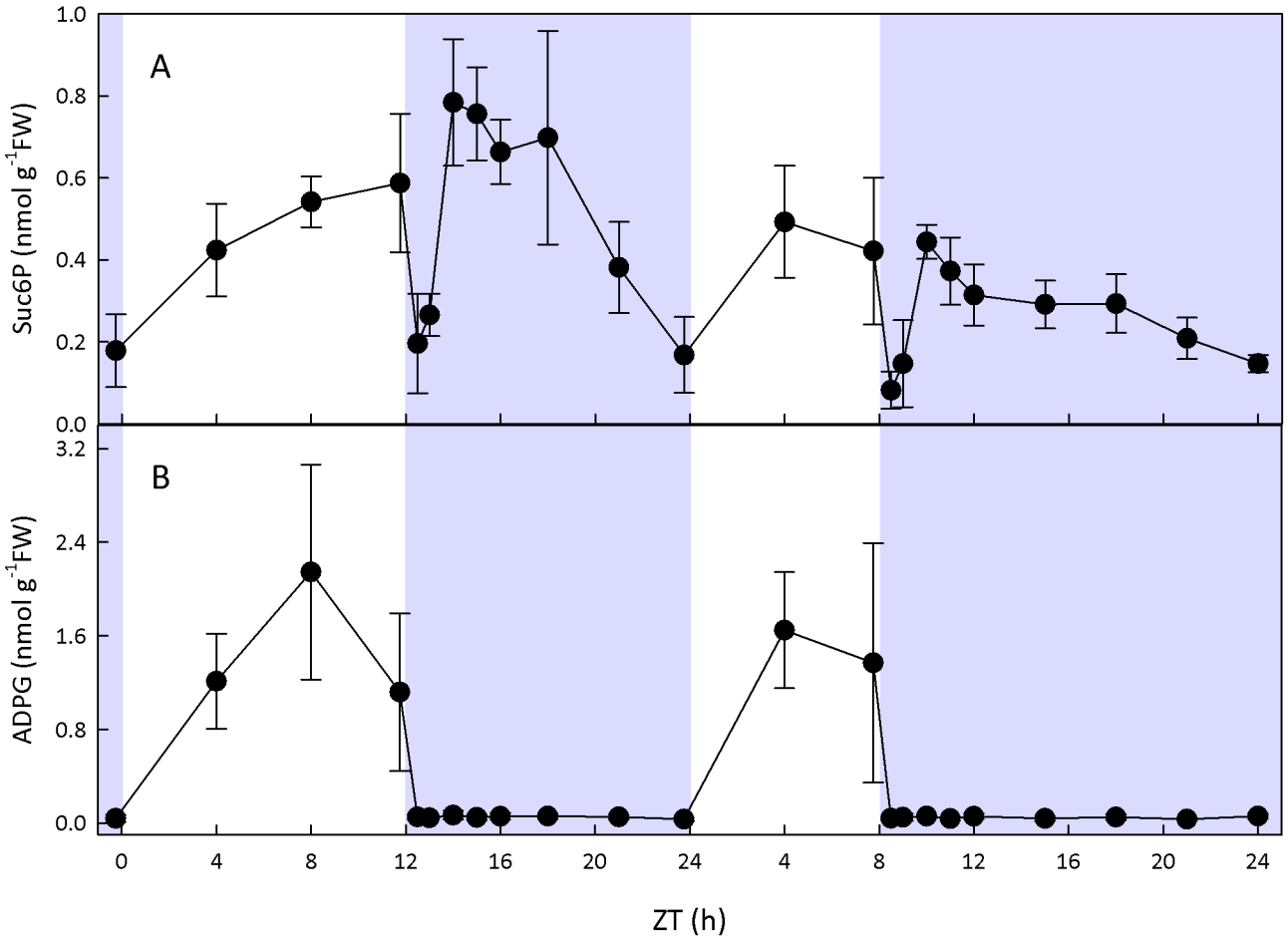

Supplemental Figure S14. Effect of an early dusk on metabolite levels in Arabidopsis leaves.

Wild type Arabidopsis Col-0 plants were grown in soil with a 12-h photoperiod for 3 weeks. Pools of five rosettes were harvested at various intervals through two sequential diurnal cycles: (i) 12 h light/12 h dark (control), and (ii) 8 h light/16 h dark (early dusk treatment) for measurement of: (A) Suc6P, (B) ADPG. Data are mean ± S.D. (n=4).

Supplemental Table S1. Effect of Tre6P and trehalose on the *in vitro* activity of enzymes involved in starch degradation.

Recombinant potato glucan, water dikinase (GWD), Arabidopsis SEX4 phosphoglucan phosphatase, and Arabidopsis β-amylase 3 (BAM3) were assayed in the presence of up to 1 mM Tre6P or 1 mM trehalose. GWD and PWD were assayed using crystallised maltodextrin (MD_{cryst}). The A-type allomorph of MD_{cryst} is more compact, consisting of flat layers of double helices, which is a typical feature of cereal starch, whereas the B-type has a more complex structure in which six double helices surround a central cavity that is filled with water. The transitory starch in Arabidopsis and potato leaves belongs to the B-type (Gallant et al., 1997; Gérard et al., 2001; Hejazi et al., 2008). Activities in the presence of Tre6P or trehalose are expressed as percentages of the activity in control reactions with no addition: (i) GWD, 69 nmol min^{-1} mg^{-1}protein; (ii) SEX4, 1.9 % P released min^{-1} μg^{-1} protein; (iii) BAM3, 29 µmol maltose min^{-1} mg^{-1}protein. Data represent single reaction rate determinations derived by linear regression of measurements from at least four different time points. *nd*, not determined.

Addition	**Concentration** *µM*	**Enzyme activity** *% of control*		
		GWD	SEX4	BAM3
None	0	(100)	(100)	(100)
Tre6P	10	122	*nd*	*nd*
Tre6P	50	107	*nd*	98
Tre6P	100	97	95	98
Tre6P	500	98	94	95
Tre6P	1000	105	*nd*	88
Trehalose	100	*nd*	96	112
Trehalose	500	109	94	110
Trehalose	1000	110	*nd*	108